LRRC8A IS ESSENTIAL FOR SWELLING ACTIVATED CHLORIDE CURRENT AND FOR REGULATORY VOLUME DECREASE IN ASTROCYTES

Formaggio Francesco[1,2], Saracino Emanuela[3], Mola Maria Grazia[5], Rao Shreyas Balachandra[4], Amiry-Moghaddam Mahmood[4], Muccini Michele[2], Zamboni Roberto[3], Nicchia Grazia Paola[5,6], Caprini Marco[1,2]*, Benfenati Valentina[2,3]*

1 Laboratory of Human and General Physiology, Department of Pharmacy and Biotechnology (FaBiT), University of Bologna, Via S. Donato 19/2, 40127 Bologna, Italy.

2 Institute for the Study of Nanostructured Materials, National Research Council of Italy (CNR-ISMN) Via P. Gobetti 101, 40129, Bologna, Italy.

3 Institute for the Organic Synthesis and Photoreactivity, National Research Council of Italy (CNR-ISOF) Via P. Gobetti 101, 40129, Bologna, Italy.

4 Department of Molecular Medicine, Institute of Basic Medical Sciences, University of Oslo, Post box 1105, Blindern, 0317, Oslo, Norway;

5 Department of Bioscience, Biotechnologies and Biopharmaceutics, Centre of Excellence in Comparative Genomics, University of Bari "Aldo Moro", Bari, BA, Italy

6 Department of Neuroscience, Albert Einstein College of Medicine, Yeshiva University, New York, Bronx, NY, USA

E-mail *corresponding senior authors:

valentina.benfenati@isof.cnr.it, Institute for the Organic Synthesis and Photoreactivity, National Research Council of Italy (CNR-ISOF) Via P. Gobetti 101, 40129, Bologna, Italy.

m.caprini@unibo.it, Laboratory of Human and General Physiology, Department of Pharmacy and Biotechnology (FaBiT), University of Bologna, Via S. Donato 19/2, 40127 Bologna, Italy.

Abbreviations: AM, acetoxymethyl; B, biotinylated; Cb, Cerebellum; DAPI, 4',6-diamidino-2-phenylindole; FCx, Frontal Cortex; GAPDH, Glyceraldehyde 3-phosphate dehydrogenase; GFAP, Glial Fibrillary Acidic Protein; GFP, Green Fluorescent Protein; HCT 116, Human colon carcinoma cell line; Hipp, Hippocampus; IB, immunoblot; KD, knockdown; Mb, Middle brain; NDS, Normal Donkey Serum; NKCC1, Na-K-Cl co-transporter-1; NT, untransfected; P, precipitation product; PBS, Phosphate-buffered saline; PCx, Parietal Cortex; PM, plasma membrane; Post-IP, post-precipitation product; Pre-IP, total lysate; siRNA, short interference RNA; St, Substantia Nigra; T, transfected; Vh, holding potential

Abstract

Consolidated evidence indicates that astroglial cells are critical in the homeostatic regulation of cellular volume by means of ion channels and aquaporin 4. Volume Regulated Anion Channel (VRAC) is the chloride channel that is activated upon cell swelling and critically contributes to cell volume regulation in astrocytes. The molecular identity of VRAC have been recently defined, revealing that it belongs to the Leucine-Rich Repeat-containing 8 (LRRC8) protein family. However, there is a lack of evidence demonstrating that LRRC8A underpins VRAC currents in astrocyte. Nonetheless, a direct evidence of the role of LRRC8A in astrocytic Regulatory Volume Decrease (RVD), remains to be proved. Here, we aim to bridge this gap in knowledge by combining RNA interference specific for LRRC8A with patch-clamp analyses and a water permeability assay. We demonstrated that LRRC8A molecular expression is essential for swelling-activated chloride current via VRAC in primary cultured cortical astrocytes. Knocking Down (KD) LRRC8A with a specific siRNA, abolished the recovery of the cell volume after swelling induced by hypotonic challenge. In addition, immunoblotting, immunofluorescence, confocal imaging and immunogold electron microscopy demonstrated that LRRC8A is expressed in the plasma membrane of primary cortical astrocytes, and, *in situ*, also in astrocytes at the perivascular interface with endothelial cells. Collectively, our results suggest that LRRC8A is an essential sub-unit of VRAC and a key factor for astroglial volume homeostasis.

KEYWORDS: Edema, Ion channels, VRAC, Neurotoxicity, Central Nervous System, Volume regulation

INTRODUCTION

The ability of brain cells to regulate their volume is an essential homeostatic function. The ion and molecular composition of the extracellular or intracellular milieu constantly change during and after neuronal network activity (1). Consequently, osmotic-driven water fluxes continuously change the cell volume. It is established that astrocytes are the cells critically involved in homeostatic volume regulation in the brain (2, 3). The characteristic star-like shape of astrocytes, with multiple processes contacting synapses and microvessels enable them to tightly regulate the composition of the interstitial compartment and to maintain hydrosaline homeostasis of the Central Nervous System (CNS). To accomplish this task, astrocytes are equipped with a variety of channels, that transport ions, organic osmolytes and water across the plasma membrane. Water flux is mediated osmotically majorly through channel aquaporin-4 (AQP4) (4-6). Among ion channels, it has been shown that VRAC activation is critical to volume regulating mechanisms in astrocytes, that are initiated to counteract cell swelling, termed Regulatory Volume Decrease (RVD) (7-11). Upon cell swelling, VRAC activation leads to the release of chloride (Cl^-) and organic osmolytes (such as taurine, glutamate and aspartate) (12-25) that is paralleled by the extrusion of intracellular K^+ (16, 20). Ion efflux in turn generates the osmotic gradient needed to drive water efflux that in turn enable the recovery of physiological cell volume (8). Several works have defined the biophysical properties of VRAC currents, including astrocytes *in vitro* and *in situ* (26-30). VRAC is activated mainly by hypotonicity-induced cell swelling. However, the capability of ATP and purinergic stimulation inducing VRAC-mediated release of glutamate and taurine in non-swollen cells have been reported (23, 31-33). The rectification profile shows moderate outward rectification (9, 34, 35), while the time dependency of VRAC current is fast activating, non-inactivating at hyperpolarizing voltages but inactivating at voltages above +40 mV (35, 36). The ability of VRAC of releasing gliotransmitters (such as glutamate) has been reported. The latter functionality associated with the ability of ATP to promote VRAC-mediated gliotransmitter release lead to the hypothesis that VRAC might be involved in physiological modulation of synaptic activity by astrocytes or, at least, in neuroglial communication (7, 23, 37-38). The capability of releasing glutamate and aspartate has been the basis for the investigation of the implication of VRAC in the mechanisms of pathophysiologies related to dys-homeostasis of brain volume such as edema occurring after stroke, ischemia, trauma (15, 19, 24). Pharmacological studies demonstrate the involvement of VRAC in excitotoxic glutamate/aspartate release *in vivo* (24, 39-41). However, all the inhibitors of VRAC currents or VRAC mediated amino acid release failed so far in both selectivity and specificity (7, 22, 42). In this context, the lack of knowledge on molecular identity of VRAC hampered direct proof of the physiological and pathophysiological role of VRAC. Recently, two groups established that the leucine rich repeat containing 8 family member A (LRRC8A) is an essential sub-unit of VRAC and must assemble with at least one of the other four members of the family (LRRC8B-E) to form a functional chloride channel (43-45). Since the breakthrough

discovery that LRRC8A is an essential molecular constituent of VRAC, several studies reported correlation between expression of LRRC8A and the function of VRAC in different cell types (46-50). In astrocytes, the group of Prof. Mongin was the first to report the expression of LRRC8A mRNA in primary rat astrocytes using real-time PCR, demonstrating the essential role of LRRC8A/VRAC in mediating the swelling-activated release of taurine and aspartate (51). However, electrophysiological evidence that LRRC8A mediates VRAC-currents in astrocyte, as well the proof of its involvement in astrocytic RVD, are still lacking. Here we report evidence that LRRC8A protein is expressed in cortical rat astrocyte membrane *in vitro* and in the mouse brain, where it is particularly abundant in astrocytic processes facing blood vessels. Moreover, using RNA interference, we demonstrate that LRRC8A is fundamental for hypotonicity-induced astroglial VRAC current and astroglial RVD *in vitro*.

MATERIALS AND METHODS

Ethics statement

All primary cell cultures were prepared at the Department of Pharmacy and Biotechnology (FABIT) of the University of Bologna. Experiments were carried on according to Italian and European Community Council guidelines for the use of laboratory animals and were approved by the Bioethical Committee of the University of Bologna (protocol n° 360/2017 PR). Every effort was made to minimize the number of animals used and their sufferings. Experiments performed on adult mice were of C57/BL6 background. Protocols relating to animal experiments were approved by University of Oslo's Animal Care and Use Committee and conform to European Council law on protection of laboratory animals.

Astrocyte primary cultures

Rat cortical astrocytes were obtained from newborn animals (Charles River, Wilmington, MA, USA) as described previously (52). Culture flasks were maintained for 2–5 weeks in an incubator at controlled temperature and pH (37° C and 5% CO_2), prior to experimental use. After 2-3 weeks, astrocytes were re-plated onto the respective substrates by enzymatically dispersion, using 0,05% trypsin-EDTA (Gibco, Thermo Fisher Scientific, Waltham, MA, USA) and seeded at the desired concentration depending on the experiment.

Cell lines

COS-7 cells were cultured in DMEM-glutamax, 10% FBS and penicillin (100-200 U/ml) - streptomycin (100 µg /ml) (Gibco, Thermo Fisher Scientific, Waltham, MA, USA). HCT 116 cell line was cultured in RPMI medium, 10% FBS and antibiotics similarly to COS-7, at 37°C 5% CO_2.

Transfection of COS-7 cells and siRNA transfection in astrocytes

The day before transfection, COS-7 cells were seeded in 60-mm Petri dishes at a density of 5-8*10^5 per dish. COS-7 were transfected with the LRRC8A/pCMV6 construct and Lipofectamine 2000 was used as transfection reagent (Thermo Fisher Scientific, Waltham, MA, USA).

For gene expression knockdown of LRRC8A, commercially gene-specific siRNA constructs were used (ON-TARGETplusSMARTpool siRNA L-090547-02-0020, Dharmacon Research, Lafayette, CO, USA). A scramble negative control was used to detect any unspecific effect of RNA interference method of gene silencing, while Alexa-fluor 555-labeled to detect transfection efficiency, which routinely reached 95%. An additional negative control where astrocytes were incubated only with the transfection reagent (Lipofectamine®RNAiMAX) was

also included (CTsiRNA). Astrocytes grown to 70% confluency were transfected with the selected SiRNA (100 nM) using Lipofectamine®RNAiMAX reagent (2 µ*l*/ml, Thermo Fisher Scientific, Waltham, MA, USA) in serum-free OptiMEM. After 5 hours of incubation with siRNA/Lipofectamine complexes, media were replaced with fresh DMEM, 10% FBS. Functional assays were performed at 4-5 days post-transfection.

Antibodies

The following primary antibodies were used: GAPDH (Western Blot 1:500 from Santa Cruz Biotechnology, Dallas, TX, USA, sc-47724), LRRC8A (Western Blot 0,8 µg/ml, Immunofluorescence 8 µg/ml; Immunoelectron Microscopy 4 µg/ml, Custom), Anti-GFAP (Immunofluorescence 1:500 from Chemicon®, EMD Millipore, Billerica, MA, USA) and β actin (Western Blot 1:1000, Sigma Aldrich, Saint Louis, MO, USA, A2066). A polyclonal rabbit antibody was generated by Twin Helix, Milan, Italy, for this particular study against the intracellular loop between TMD2 and TMD3 of LRRC8A, as previously described by Prof. Jentsch's group (43). The serum was affinity-purified against the respective peptides. A peptide negative control was also included.

Immunoblot analysis and biotinylation

COS-7 cells and 3–4 weeks cultured astrocytes were used for immunoblotting experiments as described (30). Required amount of total protein lysate were separated on a polyacrylamide gel, electro-transferred onto a PVDF membrane (Thermo Fisher Scientific, Waltham, MA, USA), blocked in 5% BSA and incubated with the primary Ab at 4 C° for 12-16 hours. Membranes were then washed three times with PBS-T 0,1% and probed with the required IgG horse radish peroxidase–conjugated secondary antibodies (1:10000, Sigma Aldrich, Saint Louis, MO, USA), developed with the enhancing chemiluminescence detection system (Santa Cruz Biotechnology, Dallas, TX, U.S.A) and visualized utilizing the ChemiDoc XRS system (Bio-Rad Laboratories, Hercules, CA). For plasma membrane protein isolation, biotinylation of cell membrane protein was performed and biotinylated proteins were separated with immobilized streptavidin as previously described (53). Briefly, cultured astrocytes were washed with ice-cold phosphate-buffered saline (PBS) and then incubated with biotinamidohexanoic acid 3-sulfo-N-hydroxysuccinimide ester sodium salt to a final concentration of 25 µg/mL (Sigma Aldrich, Saint Louis, MO, USA) for 30 min at 4°C in ice-cold biotinylation buffer (50 mm sodium borate, pH 8, 150 mm NaCl). The reaction was stopped with cold Tris-HCl, pH 8.8, for 15 min. Astrocytes were subsequently harvested with RIPA buffer and spun at 14 000 g for 30 min at 4°C. Protein concentration was determined in the supernatant before and after precipitation using a Bio-Rad protein assay (Bio-Rad Laboratories, Hercules, CA, USA) and equal amounts of protein were used for the purification with streptavidin–agarose (Sigma Aldrich, Saint Louis, MO, USA), which specifically binds biotin-conjugated cell-

surface proteins. Affinity-purified protein complexes were washed three times with lysis buffer, denatured with Laemmli sample buffer (70°C for 10 min). Total lysate containing 15 µg total protein (pre-P) and post-precipitation samples (post-P), and 15 µL affinity-purified protein complexes (membrane fraction, P) were separated by sodium dodecyl sulphate–polyacrylamide gel electrophoresis (SDS–PAGE), transferred on to PVDF and probed by western blot analysis. Mouse brain tissue was dissected (n=4) and processed for protein analysis. Brain was homogenized at 4 °C using 2 mL Lysing matrix D Eppendorf tubes (MP Biomedicals, Santa Ana, CA, USA), containing lysis buffer supplemented with protease inhibitor cocktail (Roche, Basel, Switzerland). Homogenization was performed in a FastPrep FP120 Cell Disrupter (MP Biomedicals, Santa Ana, CA, USA), shaken at intervals and intermittently cooled on ice. Supernatants were subsequently spun at high centrifuge speed and stored at -80°C until downstream applications.

Electrophysiology

Whole cell recordings of swelling-activated Cl^- currents were performed in cultured astrocytes as previously described (30). Astrocytes plated in small petri dishes were mounted on an inverted microscope (Nikon Diaphot, Nikon Italy, Firenze, Italy). Currents were recorded with the patch clamp technique, in whole cell configuration (54). Patch pipettes were prepared from thin-walled borosilicate glass capillaries to obtain a tip resistance of 2–4 MΩ. Membrane currents were amplified with an EPC-7 amplifier (List Electronic, Darmstadt, Germany), and low-pass filtered at 2 kHz (3 dB) and data were acquired with a sample rate of 5 kHz. Traces were analyzed offline with pClamp 6 software (Axon Instrument, Foster City, CA, USA) and Origin 6.0, (MicroCal, Northampton, MA, USA). Experiments were performed at room temperature (22–24 °C).
Saline solutions for patch clamp experiments were prepared with salts (Sigma Aldrich, Saint Louis, MO, USA) of the highest purity grade, and deionized and sterilized water. For electrophysiological recordings the standard bath solution was (mM): 140 NaCl, 4 KCl, 2 $MgCl_2$, 2 $CaCl_2$, 10 HEPES, 5 glucose, pH 7.4 with NaOH and osmolarity adjusted to ~315 mOsm with mannitol. In order to isolate Cl^- current, the external bath perfusion, termed control saline, was (in mM): 120 CsCl, 2 $MgCl_2$, 2 $CaCl_2$, 10 TES, 5 glucose, pH 7.4 with CsOH, and osmolarity adjusted to approximately 320 mOsm with mannitol (about 60 mM). The intracellular (pipette) solution was composed of (in mM): 126 CsCl, 2 $MgCl_2$, 1 EGTA, 10 TES, pH 7.2 with CsOH, and osmolarity adjusted to approximately 300 mOsm with mannitol. The hypotonic extracellular solution of about 260 mOsm was obtained by omitting mannitol in the control solution. In order to selectively block VRAC currents, carbenoxolone was freshly added at the hypotonic solution at a concentration of 100 µM (CBX 100 µM).

Brain sections and immunofluorescence

The animals were transcardially perfusion-fixed for 15 min with 4 % formaldehyde and post-fixed overnight. The sections (section thickness 20 µm) after a two-step washing in PBS, were blocked in 10% NDS 1% BSA, 0,5% Triton X-100 in PBS and incubated overnight with primary antibodies at the desired dilution in 3% NDS 1% BSA, 0,5% Triton X-100 in PBS. Brain sections were then incubated with secondary antibody conjugated to different fluorophores, depending on the staining. Lectin staining was performed during secondary antibody incubation with DyLight 649 labeled Lycopersicon Esculentum Lectin (Vectors Laboratories, Burlingame, CA, USA). After washing, nuclei were stained using Hoechst 33258 (Thermo Fisher Scientific, Waltham, MA, USA) and mounted on the coverslips with Fluoromount (Molecular Probes, Eugene, OR, USA). Images of brain sections were captured using a Zeiss SP1/MP (Carl Zeiss, Oberkochen, Germany) confocal microscope and processed using Zeiss Imaging software. The microscope was equipped with a 400 nm diode, 488 nm Ar^+ and 543 nm He-Ne lasers as exciting sources. For COS-7 and astrocytes immunofluorescence experiments, cells were seeded on coverslips after treatment with poly-D-lysine; after 48 hours, cells were fixed and probed with the primary antibodies as described above. The next day cells were incubated with a secondary antibody, stained with DAPI and analyzed using a Zeiss SP1/M confocal microscope. In experiments conducted with control antigen, antibody was pre-adsorbed by incubation with immunizing peptide 1 h at room temperature (3 µg peptide/1 µg antibody). Results are representative of 4 independent experiments.

Immunogold histochemistry

For immunogold electron microscopy experiment, animals were perfusion-fixed as previously described (55, 56). Tissue blocks of 1x1 mm from parietal cortex were dissected out and cryoprotected in gradient glycerol solution (10%, 20%, 30%). The samples were then immersed in liquid propane (cooled to -170 °C) in a cryofixation unit (Reichert KF80, Wien, Austria), incubated 0.5% uranyl acetate dissolved in anhydrous methanol at -90 °C. The temperature was gradually increased to -45 °C, in 4 °C/h steps. Specimens were washed with anhydrous methanol and infiltrated with Lowicry LHM20 resin at -45 °C with a progressive increase in the ratio of resin to methanol. Polymerization was performed with UV light (λ 360 nm) for 48 h. Ultrathin sections (80-100 nm) were obtained by using an ultrotome (Reichert Ultracut S, Leica) and the tissues were on 300 mesh grids. Tissue sections were incubated overnight with anti-LRRC8A primary antibody. The following day, tissue sections were stained with secondary antibody (1:20 dilution), coupled to 15 nm colloidal gold particles. After the sections were rinsed and contrasted with uranyl acetate (1%) and lead citrate (0,3%) for 90 s each. Labeled sections were analyzed with a TECNAI 12 transmission electron microscope at 80 kV (FEI, Hillsboro, OR, USA). Data were compared, as control, with immunizing peptide negative control.

Fluorescence-quenching assay

Astrocytes were seeded on black, clear bottom 96-well-plates (Corning, NY, USA) at a density of 12,000 cells per well and water permeability assay was performed 24 h after plating. 80-85% confluent cells were washed with DPBS and incubated at 37 °C for 45 min with 10 μM of membrane permeable calcein-AM (Thermo Fisher Scientific, Waltham, MA, USA) in complete medium, as previously described (57-58). Calcein fluorescence was recorded on a FlexStation3 plate reader equipped with an integrated liquid handling (Molecular Devices, MDS Analytical Technologies, Sunnyvale, CA, USA) module able to transfer compounds from a source plate to the assay plate during data acquisition. The resulting membrane-impermeant calcein fluorophore exhibits concentration dependent quenching by intracellular components (proteins or salts) so that acquired changes in fluorescence are directly related to changes in the cell volume. Cells were rinsed in 60 μL of isosmolar DPBS containing 1 mM calcium chloride and hypotonicity was applied 15 s after the beginning of each reading by automated addition of an appropriate volume of NaCl-free DPBS in order to achieve 60 mOsm/L osmotic gradient. Time course fluorescence data following cell mixing with hypotonic solution were acquired over a 100 s period in order to record the swelling phase and the RVD phase. Data acquisition was performed by SoftMax Pro software, and the data were analyzed with Prism (Graph Pad) software. The slope of the RVD phase was obtained by linear regression of the experimental curve. The percentage of volume recovery was calculated from the maximum level of fluorescence after exposure to hypotonic solution and the level of fluorescence reached after the RVD.

Statistical analysis

Data are expressed as the mean standard error (SE) from at least three independent experiments. The statistical analysis was performed with two-tailed Student's *t*-test and a statistically significant difference *P* was reported if $p<0.05$ or less. Analysis of variance was also performed (one-way ANOVA), followed by Newman-Keuls post hoc test for multiple comparisons. $p<0.05$ was considered statistically significant.

RESULTS

LRRC8A is expressed in the membrane of cultured rat cortical astrocytes

To investigate the expression of LRRC8A in astrocytes, we performed immunoblot analysis of proteins extracted from primary cultured cortical as previously described (52). Immunostaining for glial fibrillary acidic protein (GFAP) and the flat, polygonal morphological phenotype of the cultured cells indicated that more than 95% were type 1 cortical astrocytes (52). To this end we used a customized antibody (for details see Materials and Methods) raised against the epitope of LRRC8A, as previously described by Voss *et al.* (43). To validate the antibody specificity, we transiently transfected COS-7 with human LRRC8A. The LRRC8A antibody recognized major bands around 95 kDa in rat cortical astrocytes as well as in mouse brain, whole protein extract (Fig. 1 A, arrow). In transfected COS-7, LRRC8A antibody recognized a strong band at 95 kDa corresponding to the recombinant LRRC8A protein (43). Non-transfected COS-7 displayed a faint band at the same molecular weight (Fig. 1 A, arrow). We further validated antibody specificity, by using LRRC8A-KO HCT 116 cell line (human colorectal carcinoma cell line) kindly provided by Prof. Jentsch (43). A band at 95 kDa was detectable in WT HCT 116 cell line. It should be noted that in a range of molecular weights between 25 kDa and 180 kDa, in addition to the band at 95 kDa, the antibody recognizes also non-specific bands at ~ 45 kDa and at ~75 kDa. However, only the signal at 95 kDa was absent in LRRC8A-KO HCT 116 cell line (Fig. 1 B, arrow). The same band is the only that was upregualted in COS-7 transfected with human LRRC8A.

To gain further insight in the expression and sub-cellular localization of LRRC8A in primary astrocytes, we isolated plasma-membrane protein fraction by biotin-streptavidin method (53). Western blot analyses of the biotinylated fraction (biotinylated-streptavidin precipitated fraction, P, Fig. 1 C) indicated that the band at 95 kDa is detectable in the plasma-membrane protein fraction of primary astrocytes. Immunoblot of cytosolic protein GAPDH revealed the absence of GAPDH signal in the streptavidin P sample and ensured the consistency of the protocol. Additionally, the band at 95 kDa that we referred to LRRC8A was not detected in the streptavidin P sample, when addition of biotin was omitted (Fig. 1 C).

To further investigate on the expression and localization pattern of LRRC8A in rat cortical astrocytes, we carried out immunofluorescence protocol and confocal microscopy imaging of sub-confluent rat cortical astrocytes, co-stained for LRRC8A (red) and Glial Fibrillary Acidic Protein (GFAP, green), a specific astrocytic marker (Fig. 2 A). Single plane confocal imaging reported in Figure 2 A indicated a strong staining in astrocytes for the anti-LRRC8A. In addition, imaging of astrocytes stained for GFAP confirmed a strong labeling and the purity of the astroglial culture. Moreover, merge of GFAP and LRRC8A confocal images revealed only partial overlay signals and confirmed plasma membrane localization of the protein, although cytoplasmic expression of LRRC8A was also evident. The selectivity of the immunofluorescence signal is supported by the absence of

staining after pre-adsorption with the immunizing peptide (Supplementary information S1). We also performed immunofluorescence with LRRC8A on COS-7 cells transiently co-transfected with the human LRRC8A and Green Fluorescence Protein. As depicted by fluorescent confocal images reported in figure 2 B, strong and clear immunolabeling for LRRC8A (Fig. 2 B, red) was observed in GFP positive cells (Fig. 2 B, green). A faint but detectable signal was also noticed in the non-transfected COS-7, revealing that COS-7 endogenously express LRRC8A (Supplementary information, Fig. S2). As negative control, we stained HCT 116 KO cells with anti LRRC8A (Fig. 2 C). The absence of immunofluorescent signal in HCT 116 KO cells proved the specificity of the immunofluorescence staining observed in astrocytes and in COS-7 cells.

Expression of LRCC8A in brain astrocytes

To address the expression pattern of LRRC8A in the brain, we performed immunofluorescence and confocal microscopy, immunogold electron microscopy on adult mouse brain samples. Sagittal sections from adult mouse brain were immuno-labeled with the anti-LRRC8A and for the astrocytic marker GFAP (Fig. 3 A). Confocal microscopy images analysis revealed a strong labeling for LRRC8A (Fig. 3 A, red) in cerebral cortical astrocytes (Fig. 3 A, Cx, white arrows). Co-localization of the astrocytic marker GFAP and LRRC8A (Fig. 3 A, merge, yellow) indicated that the subunit of VRAC is highly expressed in mouse brain cortical astrocytes *in situ*, also in astrocytic endfeet enwrapping cortical blood vessels (Fig. 3 A Cx, lower pannels, white arrows). Confocal imaging of hippocampal CA1/CA3 regions from mouse brain sections stained with LRRC8A antibody and GFAP and Lectin evidenced that LRRC8A is expressed also in astrocytes cell body (Fig. 3 B) and in astrocytes endfeet facing hippocampal vessels (Fig. 3 B, arrowheads). Immunofluorescent signal was observed also in non-GFAP positive cells.

We next performed immunogold labeling and electron microscopy analysis to analyze sub-cellular localization of LRRC8A. As reported in figure 3 C, the labeling of LRRC8A immunogold particles is localized mainly at astrocytic membrane of astrocytes endfeet facing endothelial cells of the blood vessel. Pre-adsorption of the anti-LRRC8A antibody with immunizing peptide abolished the labeling of the tissue (Fig. 3 C, right panel).

LRCC8A underpins VRAC current in cultured astrocytes

To investigate whether LRRC8A is responsible for the swelling activated anion conductance in astrocytes, we performed patch-clamp analyses of hypotonic-activated chloride current on astrocytes transfected with a pool of siRNA purchased from Dharmacon (Lafayette, CO, USA). As confirmed by the western blot analysis of

astroglial whole-cell lysate, the transfection resulted in an almost complete knockdown of the signal at 95 kDa that we recognize as specific for LRRC8A (Fig. 4 A, inset, full lane western blot image reported in Supplementary S3). We also transfected primary astrocytes with a scramble negative control to detect any unspecific effect of RNA interference gene silencing (Scramble siRNA). Alexa-fluor 555-labeled was used to detect transfection efficiency, which routinely reached 95% (Supplementary information, Fig. S4).

To analyze hypotonic activated current, we applied protocols previously reported (30, 42). Accordingly, astrocytes were clamped at the holding potential (Vh) of 0 mV, next to the astrocyte zero-current potential under our experimental conditions, and stimulated with voltage ramps of 1-s duration from -80 to 80 mV (Fig. 4 A). Whole-cell membrane conductance recorded in extracellular isotonic bathing solution (Fig. 4 A, trace 1) was small in magnitude, and increased upon exposure to hypotonic solution (ΔOsm = 60 mOsm) in Scramble siRNA transfected cells (Fig. 4 A, trace 2). Of note steady-state ramp currents were inhibited by micromolar concentration of carbenoxolone (Fig. 4 A, trace 3). On the contrary, hypotonic challenge failed to elicit a significant increase in whole-cell current in LRRC8A siRNA transfected cells (Fig. 4 A, right trace).

The analyses of typical time course of current densities recorded at -80 mV and +80 mV (Fig. 4 B, black circles), revealed that VRAC response upon hypotonic challenge was elicited and reached the value of steady-state after 5 min in Scramble siRNA cells. On the contrary, VRAC failed to be activated at each time point in LRRC8A siRNA transfected cells, from the onset to the steady state (Fig. 4 B, gray squares). The inhibition of VRAC current by siRNA targeting LRRC8A was almost complete, as reflected by histogram plot of current density of hypotonic activated current reported in Figure 4 C.

To analyze if siRNA targeting LRRC8A affects biophysical properties of VRAC, the voltage- and time-dependency of VRAC was analyzed in Scramble siRNA and in LRRC8A siRNA. To this end Cl^- currents were elicited with a voltage step protocol (inset to Fig. 4 D) composed of a family of voltage steps from Vh 0 mV from -80 to +80 mV in 20 mV increments delivered every 10 sec. Hypotonic-activated voltage step currents were obtained by digital subtraction of current traces recorded before and after 5–7 min of hypotonic challenge. Consistently with VRAC biophysical profile, in Scramble siRNA the currents activated instantaneously at all voltages and did not inactivate at potentials between -40 and +40 mV. At membrane potentials positive to +40 mV the evoked currents displayed a typical time-dependent inactivation, whose rate and extent became larger at more depolarized potentials (Fig. 4 D, left trace). In LRRC8A siRNA the hypotonic-induced chloride current was negligible at each voltage applied (Fig. 4 D, right trace).

LRCC8A is involved in RVD in cultured astrocytes

We then investigated the role of LRRC8A on astrocytic RVD. In this set of experiments, Scrambled siRNA astrocytes responded to hypo-osmotic stress (60 mOsm) by a rapid volume increase culminating at ~7 s of

hypotonic stress (Fig. 5 A). Swelling was followed by a volume decrease reaching basal level at ~20 s of hypotonic stress with no changes in the swelling rates as well as the absolute volume increase when compared to CTsiRNA, indicating that water permeability was not affected in our experimental set-up. However, knocking down of LRRC8A seriously impaired RVD as indicated by the significant difference in the slope of the RVD phase when compared to Scramble siRNA (Fig. 5A, B). RVD was slower in LRRC8A siRNA cells and, in addition, the magnitude of the RVD response was strongly reduced, (Fig. 5 C) reaching a steady state at ~20 s and remained at high level throughout the observed period (Fig. 5 A). Experiments performed with 25 mOsm gradient (Supplementary information S6) gave comparable results.

DISCUSSIONS

The main findings of the presented work are as follows: i) LRRC8A is largely responsible for the hypotonic-induced chloride current in primary rat neocortical astroglial cells, called VRAC; ii) we demonstrated for the first time a crucial functional role of LRRC8A subunit in astroglial RVD; iii) we have shown the molecular expression at protein level of LRRC8A in the membrane of cultured rat cortical astrocytes; iv) the expression of LRRC8A in brain cortical and hippocampal astroglial cells is verified.

In cultured astrocytes, knocking down LRRC8A completely abolished the swelling-activated VRAC currents. Several recent studies, performed in different cell types, align with the data we reported in astrocytes, proving the importance of LRRC8A in mediating VRAC chloride current (43-44, 47-49). Moreover, Hyzinski-García *et al.* reported for the first time that LRRC8A largely underpins VRAC-mediated release of taurine, aspartate and glutamate in cultured astrocytes, occurring in response to hypotonic challenge (51). However, the involvement of LRRC8A in astroglial swelling activated chloride current of VRAC was not trivial. Indeed, two different studies reported that LRRC8A might be not essential in the swelling-induced anionic currents in the HeLa cell line and human retinal pigment epithelium (46, 59). These findings raise the importance of electrophysiological correlation between the molecular expression of LRRC8A in astrocytes and the functional activation of VRAC chloride current in the same cells, as we have demonstrated in cultured astrocytes by using specific siRNA for LRRC8A. Interestingly, the KD of LRRC8A completely abolished VRAC conductance and current density at any voltage applied. Also, the onset of the small residual current observed in response to hypotonic challenge is delayed and it lacks the time and voltage dependency typical of VRAC (Fig. 4 D). The current density of hypotonic induced chloride currents are not significantly different from those of isotonic current. These results are in line with studies indicating that LRRC8A is an essential subunit of chloride current mediated by VRAC (43-44, 47-50).

LRRC8A KD astrocytes exhibit only a partial recovery of the initial volume after hypotonic challenge, which correlates with a strong decrease in their RVD magnitude. These data indicate the significant contribution of LRRC8A subunit to astrocytic RVD. Since the discovery that LRRC8A is an essential sub-unit of VRAC (43, 44), this is the first study that provides direct functional and molecular evidence on the relevance of LRRC8A subunit of VRAC in astroglial RVD. Indeed, previous description of involvement of VRAC in astrocytic RVD was based on pharmacological evidence (7, 8, 22). However, VRAC inhibitors, such as Carbenoxolone (42), DCPIB (60) and Tamoxifen are also inhibiting other ion channels such as Connexins, Purinergic Receptor, Pannexin or two–P-domain potassium conductance (61-67).

Reported here RVD rates are approximately one order of magnitude faster than in previous publications in astrocytes using a variety of techniques, including the same calcein quenching approach, 3D confocal reconstruction, and Coulter sizing (23, 68, 69, 70).

As discussed in detail in the manuscript by Mola *et al.* 2016 (58), this discrepancy could be dependent on different experimental performing and recording conditions, such as the perfusion rate and acquisition time.

A previous study (51) has demonstrated that LRRC8A siRNA knockdown suppresses hypo-osmotic medium-induced amino acid release that have been causally linked to RVD in astrocytes (12, 14-17, 19, 20, 22, 23). However, direct evidence on the correlation between expression of LRRC8A and astroglial RVD have never been proved. The data we reported showing that RVD is abolished in LRRC8A siRNA transfected astrocytes are in line with studies provided by Hyzinski-García *et al.* and by the present work. The excitatory amino acid efflux as well as chloride efflux are considered the major responsible for generating driving force for osmotic water efflux and volume recovery following cells swelling. The slight volume decrease that we observed following cell swelling, can be attributed to other mechanism, like for example NKCCl co-transporters that have been shown to contribute to RVD in astrocytes (1, 71).

LRRC8A molecular expression was demonstrated in different cell type, including retinal pigment epithelium cells (46), nodose neurons (47), and adipocytes (48). In astrocytes, Hyzinski-García *et al.* and Schober *et al.* showed relative expression levels of mRNA of LRRC8A-E subunits by quantitative RT-PCR in primary astrocytes (51, 72). In our study, we provide clear evidence that LRRC8A protein is expressed in cultured rat astrocytes plasma membrane by western blot and biotinylation assay as well as by immunofluorescence. The LRRC8A antibody recognized major bands around 95 kDa in rat cortical astrocytes, possibly correlating with a different glycosylation pattern of the protein, or to peculiar LRRC8A protein isoforms expressed by primary astroglial cells. We provide several controls for the specificity of the antibody we have used. In particular, the signal at 95 kDa recognized in astrocytes is also detectable and upregulated in COS-7 transiently transfected with LRRC8A clone and in LRRC8A-WT HCT 116 cell line. The signal at the same molecular weight is absent in protein lysates extracted from LRRC8A-KO HCT 116 cell line and it is strongly downregulated in LRRC8A

KD astrocytes. In a range of weight between 25 kDa and 180 kDa, in addition to the band at 95 kDa, the antibody recognizes also non-specific bands at ~ 45 kDa and at ~75 kDa. However, non specificity of those bands can be clearly recognizable, as they are not abolished by LRRC8A KD by siRNA and they are still present in LRRC8A-KO HCT 116 cells. Negative control experiments for the custom antibodies have also been included, including incubation with control peptide and omission of detergents in the immunofluorescence preparation. Since the anti-LRRC8A epitope is intracellular, the latter control experiment provides evidence that the signal on the plasma membrane is specific. Indeed, negligible immunofluorescent signal can be observed when the cells were not permeabilized (Supplementary information S5).

The mouse brain immunofluorescence and confocal microscopy analysis performed in this study reveals that LRRC8A is highly expressed in astrocytes, particularly in perivascular astrocytes and in the astrocytes facing pial surfaces. The presence of LRRC8A in astrocytes is demonstrated by the co-localization with the astrocytic marker GFAP. Notably, the expression of LRRC8A in non-GFAP cells indicated that the protein is also expressed in non GFAP positive cells. Immunogold electron microscopy analysis confirmed the presence of LRRC8A in plasma membranes of cortical astrocytes *in situ*, showing concentrated expression at the endfeet enwrapping blood vessels. The observed LRRC8A enrichment at the astrocytic endfeet is consistent correlated with the pathophysiological role attributed to astrocytes in brain swelling and brain edema, as a consequence of stroke, brain injury, epilepsy and hyponatremia (24, 73-76). A significant body of work indeed indicates that astroglial cells are essential for the maintenance of volume homeostasis in the brain (2, 4, 77). Astrocytes are the first cells to be exposed to osmotic changes and respond to hypo-osmotic stress (4, 75). VRAC activation following cell swelling triggers and sustains the driving force for RVD since in resting conditions the membrane potential of astrocytes is more negative that of neurons, approximately -80 mV (7). Moreover, astrocytes actively accumulate Cl^- due to the high expression and activity of NKCC1 (78), leading to an equilibrium potential of -40 mV for Cl^-. Thus, activation of VRAC would consequently mediate an efflux of Cl^-, providing the driving force for K^+ to leave the cell, followed by obligated osmotic water (8, 11).

We have previously demonstrated that functional and physical interaction between AQP4 and TRPV4 occurs in astrocytes *in vitro* and *in situ* and we suggested that the two proteins cooperate to maintain volume homeostasis in the CNS (77, 79-82). However if VRAC might be part of the same plasma membrane microdomain in the brain (67) warrants further investigation. In our previous study we have shown that the KD of AQP4 promoted a downregulation of VRAC (30). Even though VRAC has been demonstrated to be a wet channel (50, 83), here, we clearly have show that water permeability is not affected by LRRC8A KD. Further studies are required to verify the cooperation and interaction of LRRC8A with other ion channels and aquaporins *in vitro* and *in vivo*.

In conclusion, our data demonstrate that LRRC8A is an essential sub-unit of the volume-regulated anion channel in astrocytes. This work provides new molecular and functional insight into the physiological role of LRRC8A/VRAC in astrocytic RVD in vitro and clues on its expression in brain astrocytes.
Our work points to consider LRRC8A as a molecular target to improve the address pathological conditions, for which actual therapies are mostly ineffective (24). In this view further investigations on slice and in KO animals are necessary.

Acknowledgements

This work was supported by grants from the University of Bologna (RFO2016/17) to M.C. and by grant from the Italian Minister for Education, University and Research within the FIRB-Futuro in Ricerca to VB and GPN; the AFOSR Research Projects ASTROMAT (FA9550 16 1 0502) and ASTRONIR, (FA9550-17-1-0502) to VB are acknowledge. We thank the Fondazione Del Monte di Bologna e Ravenna, Italy and the Italian Minister for Education, University and Research within the FIRB-Futuro in Ricerca (RBFR12SJA8_001; RBFR12SJA8_002), for providing the F.F. and E.S. PhD fellowship.
Thanks to Alessia Minardi for her assistance in astrocytes preparation and to Bjørg Riber, Karen Marie Gujord and Nadia Skauli for technical assistance and Wilson R. Adams, Dept. Biomedical Engineering, Vanderbilt University, Nashville, TN, USA, for the English proofreading of the manuscript. Special thanks to Prof. Stefano Ferroni, University of Bologna, Italy, for technical assistance in patch-clamp experiments, and Prof. Thomas Jentsch for kindly provide the HCT 116 LRRC8A-KO cell line.

Authors contribution

F.F. designed research studies, planned and performed the molecular, immunofluorescence and electron microscopy experiments and their analysis, performed electrophysiological recordings and analysis, wrote the manuscript. E.S. analyzed electrophysiological data, wrote the manuscript. M.M.G. performed water permeability measurements and analysis. R.S.B. performed immunofluorescence and electron microscopy experiments. M.M., Z.R., A.M.M. and N.G.P contributed reagents, materials, and analysis tools critically revised the manuscript. M.C. and V.B. conceived, designed and supervised the project, wrote the paper. All authors read and approved the final manuscript.

Figure 1. LRRC8A expression in rat cortical astrocytes A) Immunoblot of total astrocytic protein lysate. Western blot analyses of whole cell extract from pure cultured astroglial cells, whole mice brain, untransfected

(NT) COS-7 cells and transfected (T) with human LRRC8A, by using anti-LRRC8A antibody. A band around 95 kDa is displayed by astrocytes and COS-7 transfected with LRRC8A. **B)** HCT WT cell line expressing LRRC8A. The signal displays a band at 95 kDa which is absent in the LRRC8A KO HCT. **C)** Western blot of membrane proteins purified by using biotinylation assay. Samples obtained before (Pre-P) and after (Post-P) streptavidin precipitation (P) are also included. The precipitation (P) lane displayed the same band observed at 95 kDa in A, confirming the membrane expression of LRRC8A. The band is absent when biotin is omitted. GAPDH is absent in P (membrane) fraction.

Figure 2. LRRC8A localization in rat cortical astrocytes A) Single plane confocal immunofluorescence image of primary rat cortical astrocytes co-immunolabeled for Glial Fibrillary Acidic Protein (GFAP, green) and LRRC8A (red). Immunofluorescence analysis of LRCC8A displays a strong specific signal in astrocytes. The merge of the two images revealed that LRRC8A is only partially colocalized with GFAP (yellow). **B)** Single plane confocal immunofluorescence image of low confluence COS-7 cells co-transfected with LRRC8A (red) and GFP (green). Note overlapping of the two signals (merge). **C)** Immunofluorescence of HCT WT and KO stained with the same LRRC8A antibody. The immunofluorescent signal of LRRC8A is absent in the LRRC8A-KO line. Scale: 50 µm

Figure 3. LRRC8A expression in mouse brain A) Single plane confocal immunofluorescence images of sagittal section of mouse brain cerebral cortex (Cx), co-stained with anti-GFAP (green), anti-LRRC8A (red). Note the staining at astrocytic end feet enwrapping blood vessels (white arrows) Scale: 40 µm. **B)** Single plane confocal immunofluorescence images of sagittal section of mouse brain hippocampus (CA1/CA3), co-stained with anti-GFAP (left, green), anti-LRRC8A (middle panel, red) and merged image with DAPI (white) and Lectin (blue) (right panel). Scale: 20 µm. **C)** Immunogold electron microscopy analysis of LRRC8A expression in the cerebral cortex. High magnification images of two different blood vessels of cerebral cortex. Astrocytic endfeet is labeled with immunogold particles reflecting the expression of LRRC8A. Incubation with immunizing peptide abolished the signal (LRRC8A Ag, right panel). E: endothelial cell, L: Lumen. Scale: 500 nm.

Figure 4. VRAC current is abolished in astrocytes knockdown (KD) for LRRC8A A) Western blot analysis of astrocytes transfected with LRRC8A siRNA and Scramble siRNA (inset). Note the nearly absence of LRRC8A signal in LRRC8A siRNA astrocytes. Representative current traces mediated by VRAC in Scramble siRNA (left) and LRRC8A siRNA elicited with a stimulation protocol shown in the inset under extracellular isotonic solution (1), at the maximal current level following hypotonic challenge (2), after addition of

carbenoxolone (CBX) (3) to the hypotonic saline. Current traces were recorded using Cs^+ containing isotonic intracellular solution upon perfusion with extracellular saline (Isotonic), following hypotonic challenge (Hypotonic; Δ = −60 mOsm/kg) and after addition of 100 μM carbenoxolone, a specific VRAC inhibitor. **B)** Time course of swelling-induced VRAC activation. Cells were swollen by exposure to a 260 mOsm external solution. Each data point indicate the current monitored at +80 mV (top curves) and -80 mV (bottom curves). **C)** Histogram of hypotonicity-activated current density at -80 and +80 mV in astrocytes challenged as in **(A)**. Quantitative analysis was obtained by point-to-point digital subtraction, in Scramble siRNA astrocytes (n = 10) and LRRC8A siRNA cells (n = 13) Data are means ± SE. ***p < 0.001 compared to Scramble siRNA. **D)** Current traces evoked with a voltage-step protocol (inset), obtained by digital subtraction of currents after maximal activation of VRAC with hypotonic saline and those elicited in isotonic condition, after reaching the maximum response in hypotonicity. Scramble siRNA is depicted on the left and LRRC8A siRNA on the right.

Figure 5. **LRRC8A knockdown by siRNA significantly affect RVD kinetic in rat astrocytes. (A)** Osmotically-induced volume changes recordered by calcein quenching method in primary rat astrocytes treated with CTsiRNA, Alexa siRNA, Scramble siRNA and LRRC8A siRNA. The arrow indicates the addition of a hypotonic solution (ΔOsm = 60 mOsm/L). **(B)** Histogram of the mean ± SE values of 1/slope values of the RVD phase of the indicated cells calculated by linear regression of the experimental data. (C) Histogram showing the mean ± SE of the extent of volume recovery (in percent). **P < 0.005; *P < 0.05; n = 12 for LRRC8A siRNA; n = 13 for Alexa siRNA; n = 14 for CTsiRNA; n = 16 Scramble siRNA.

REFERENCES

1. Benfenati V., Ferroni S. (2010) Water transport between CNS compartments: functional and molecular interactions between aquaporins and ion channels. *Neuroscience***168,** 926-40
2. Simard M., Nedergaard M. (2004) The neurobiology of glia in the context of water and ion homeostasis. *Neuroscience***129,** 877-96
3. Somjen G. G. (2002) Ion regulation in the brain: implications for pathophysiology. *Neuroscientist***8,** 254–267
4. Amiry-Moghaddam M., Ottersen OP. (2003) The molecular basis of water transport in the brain. *Nat. Rev. Neurosci.***4,** 991-1001
5. Pasantes-Morales H., Lezama R.A., Ramos-Mandujano G., Tuz K.L. (2006) Mechanisms of cell volume regulation in hypo-osmolality. *Am. J. Med.***119,** S4-11
6. Pasantes-Morales H., Cruz-Rangel S. (2010) Brain volume regulation: osmolytes and aquaporin perspectives. *Neuroscience***168,** 871-84
7. Mongin A.A. (2016) Volume-regulated anion channel: a frenemy within the brain. *Pflugers Arch.***468,** 421-41
8. Hoffmann E.K., Lambert I.H., Pedersen S.F. (2009) Physiology of cell volume regulation in vertebrates. *Physiol. Rev.***89,** 193-277
9. Nilius B., Eggermont J., Voets T., Buyse G., Manolopoulos V., Droogmans G. (1997) Properties of volume-regulated anion channels in mammalian cells. *Prog. Biophys. Mol. Biol.***68,** 69-119
10. Okada Y. (1997) Volume expansion-sensing outward-rectifier Cl- channel: fresh start to the molecular identity and volume sensor. *Am. J. Physiol.***273,** 755-89
11. Lang F., Busch G.L., Ritter M., Völkl H., Waldegger S., Gulbins E., Häussinger D. (1998) Functional significance of cell volume regulatory mechanisms. *Physiol. Rev.***78,** 247-306
12. Kimelberg HK, Rutledge E, Goderie S, Charniga C. (1995) Astrocytic swelling due to hypotonic or high K^+ medium causes inhibition of glutamate and aspartate uptake and increases their release. *J Cereb. Blood Flow Metab.***15,** 409-16
13. Pasantes-Morales H., Moran J., Schousboe A. (1990) Volume-sensitive release of taurine from cultured astrocytes: properties and mechanism. *Glia***3,** 427-32
14. Jackson P.S., Strange K. (1993) Volume-sensitive anion channels mediate swelling-activated inositol and taurine efflux. *Am. J. Physiol.***265,** 489-500
15. Kimelberg H.K., Mongin A.A. (1998) Swelling-activated release of excitatory amino acids in the brain: relevance for pathophysiology. *Contrib. Nephrol.***123,** 240-57

16. Vitarella D., DiRisio D.J., Kimelberg H.K., Aschner M. (1994) Potassium and taurine release are highly correlated with regulatory volume decrease in neonatal primary rat astrocyte cultures. *J. Neurochem.***63,** 1143-9
17. Rutledge E.M., Aschner M., Kimelberg H.K. (1998) Pharmacological characterization of swelling-induced D-[3H]aspartate release from primary astrocyte cultures. *Am. J. Physiol.***274,** 1511-20
18. Crepel V., Panenka W., Kelly M.E., MacVicar B.A. (1998) Mitogen-activated protein and tyrosine kinases in the activation of astrocyte volume-activated chloride current. *J. Neurosci*.**18,** 1196–1206
19. Feustel P.J., Jin Y., Kimelberg H.K. (2004) Volume-regulated anion channels are the predominant contributors to release of excitatory amino acids in the ischemic cortical penumbra. *Stroke***35,** 1164-8
20. Olson J.E., Li G.Z. (1997) Increased potassium, chloride, and taurine conductances in astrocytes during hypoosmotic swelling. *Glia***20,** 254–261
21. Nedergaard M., Takano T., Hansen A.J. (2002) Beyond the role of glutamate as a neurotransmitter. *Nat. Rev. Neurosci*.**3,** 748-55
22. Abdullaev I.F., Rudkouskaya A., Schools G.P., Kimelberg H.K., Mongin A.A. (2006) Pharmacological comparison of swelling-activated excitatory amino acid release and Cl- currents in cultured rat astrocytes. *J. Physiol*.**572,** 677-89
23. Takano T., Kang J., Jaiswal J.K., Simon S.M., Lin J.H., Yu Y., Li Y., Yang J., Dienel G., Zielke H.R., Nedergaard M. (2005) Receptor-mediated glutamate release from volume sensitive channels in astrocytes. *Proc. Natl. Acad. Sci. U. S. A.***102,** 16466-71
24. Kimelberg H. K. (2005) Astrocytic swelling in cerebral ischemia as a possible cause of injury andtarget for therapy. *Glia***50,** 389–397
25. Akita T, Okada Y. (2014) Characteristics and roles of the volume-sensitive outwardly rectifying (VSOR) anion channel in the central nervous system. *Neuroscience***275,** 211–231.
26. Jentsch T.J., Stein V., Weinreich F., Zdebik A. A. (2002) Molecular structure and physiological function of chloride channels. *Physiol. Rev*.**82,** 503–568
27. Parkerson K.A. and Sontheimer H. (2003) Contribution of chloride channels to volume regulation of cortical astrocytes. *Am. J. Physiol. Cell Physiol.***284,** 1460–1467.
28. Parkerson K.A. and Sontheimer H. (2004) Biophysical and pharmacological characterization of hypotonically activated chloride currents in cortical astrocytes. *Glia***46,** 419-36
29. Walz W. (2002) Chloride/anion channels in glial cell membranes. *Glia***40,** 1-10
30. Benfenati V., Nicchia G.P., Svelto M., Rapisarda C., Frigeri A., Ferroni S. (2007) Functional down-regulation of volume-regulated anion channels in AQP4 knockdown cultured rat cortical astrocytes. *J. Neurochem*.**100,** 87-104

31. Akita T., Fedorovich S.V., Okada Y. (2011) Ca^{2+} nanodomain-mediated component of swelling-induced volume-sensitive outwardly rectifying anion current triggered by autocrine action of ATP in mouse astrocytes. *Cell. Physiol. Biochem*.**28,** 1181-90
32. Mongin A.A., Kimelberg H.K. (2002) ATP potently modulates anion channel-mediated excitatory amino acid release from cultured astrocytes. *Am. J. Physiol. Cell. Physiol*.**283,** C569–C578
33. Mongin A.A, Kimelberg H.K. (2005) ATP regulates anion channel-mediated organic osmolyte release from cultured rat astrocytes via multiple Ca^{2+}-sensitive mechanisms. *Am. J. Physiol. Cell. Physiol*.**288,** C204–C213
34. Strange K., Emma F., Jackson P.S. (1996) Cellular and molecular physiology of volume-sensitive anion channels. *Am. J. Physiol*.**270,** C711-30
35. Okada Y., Petersen C.C., Kubo M., Morishima S., Tominaga M. (1994) Osmotic swelling activates intermediate-conductance Cl^- channels in human intestinal epithelial cells. *Jpn. J. Physiol*.**44,** 403 9
36. Voets T., Droogmans G., Nilius B. (1997) Modulation of voltage-dependent properties of a swelling-activated Cl^- current. *J. Gen. Physiol*.**110,** 313-25
37. Parpura V., Heneka M.T., Montana V., Oliet S.H., Schousboe A., Haydon P.G., Stout R.F Jr., Spray D.C., Reichenbach A., Pannicke T., Pekny M., Pekna M., Zorec R., Verkhratsky A. (2012) Glial cells in (patho)physiology. *J. Neurochem*.**121,** 4–27
38. Fisher S.K., Heacock A.M., Keep R.F., Foster D.J. (2010) Receptor regulation of osmolyte homeostasis in neural cells. *J. Physiol*.**588,** 3355-64
39. Phillis J.W., Song D., O'Regan M.H. (1997) Inhibition by anion channel blockers of ischemia-evoked release of excitotoxic and other amino acids from rat cerebral cortex. *Brain Res*.**758,** 9–16
40. Phillis J.W., Song D., O'Regan M.H. (1998) Tamoxifen, a chloride channel blocker, reduces glutamate and aspartate release from the ischemic cerebral cortex. *Brain Res*.**780,** 352–355
41. Kimelberg H.K., Jin Y., Charniga C., Feustel P.J. (2003) Neuroprotective activity of tamoxifen in permanent focal ischemia. *J. Neurosurg*.**99,** 138–142
42. Benfenati V., Caprini M., Nicchia G.P., Rossi A., Dovizio M., Cervetto C., Nobile M., Ferroni S. (2009) Carbenoxolone inhibits volume-regulated anion conductance in cultured rat cortical astroglia. *Channels (Austin)***3,** 323-36
43. Voss F.K., Ullrich F., Münch J., Lazarow K., Lutter D., Mah N., Andrade-Navarro M.A., von Kries J.P., Stauber T., Jentsch T.J. (2014) Identification of LRRC8 heteromers as an essential component of the volume-regulated anion channel VRAC. *Science***344,** 634-8

44. Qiu Z., Dubin A.E., Mathur J., Tu B., Reddy K., Miraglia L.J., Reinhardt J., Orth A.P., Patapoutian A. (2014) SWELL1, a plasma membrane protein, is an essential component ofvolume-regulated anion channel. *Cell***157,** 447-45
45. Jentsch T.J. (2016) VRACs and other ion channels and transporters in the regulation of cell volume and beyond. *Nat Rev Mol Cell Biol.***17,** 293-307
46. Milenkovic A., Brandl C., Milenkovic V.M., Jendryke T., Sirianant L., Wanitchakool P., Zimmermann S., Reiff C.M., Horling F., Schrewe H., Schreiber R., Kunzelmann K., Wetzel C.H., Weber B.H. (2015) Bestrophin 1 is indispensable for volume regulation in humanretinal pigment epithelium cells. *Proc. Natl. Acad. Sci. U. S. A.***112,** E2630-9
47. Wang R., Lu Y., Gunasekar S., Zhang Y., Benson C.J., Chapleau M.W., Sah R., Abboud F.M. (2017) The volume-regulated anion channel (LRRC8) in nodose neurons is sensitive to acidic pH. *J.C.I. Insight***2,** 1-18
48. Zhang Y., Xie L., Gunasekar S.K., Tong D., Mishra A., Gibson W.J., Wang C., Fidler T., Marthaler B., Klingelhutz A., Abel E.D., Samuel I., Smith J.K., Cao .L, Sah R. (2017) SWELL1 is a regulator of adipocyte size, insulin signalling and glucose homeostasis. *Nat. Cell. Biol*.**19,** 504-517
49. Yamada T., Wondergem R., Morrison R., Yin V.P., Strange K. (2016) Leucine-rich repeat containing protein LRRC8A is essential for swelling-activated Cl- currents and embryonic development in zebrafish. *Physiol. Rep*.**4,** 1-11
50. Gaitán-Peñas H., Gradogna A., Laparra-Cuervo L., Solsona C., Fernández-Dueñas V., Barrallo-Gimeno A., Ciruela F., Lakadamyali M., Pusch M., Estévez R. (2016) Investigation ofLRRC8-Mediated Volume-Regulated Anion Currents in Xenopus Oocytes. *Biophys J*.**111**, 1429-1443
51. Hyzinski-García M.C., Rudkouskaya A., Mongin A.A. (2014) LRRC8A protein is indispensable for swelling-activated and ATP-induced release of excitatory amino acids in rat astrocytes. *J. Physiol*.**592,** 4855-62
52. Ferroni S., Marchini C., Schubert P., Rapisarda C. (1995) Two distinct inwardly rectifying conductances are expressed in long term dibutyryl-cyclic-AMP treated rat cultured cortical astrocytes. *FEBS Lett.***367,** 319-25
53. Benfenati V, Caprini M, Nobile M, Rapisarda C, Ferroni S. (2006) Guanosine promotes the up-regulation of inward rectifier potassium current mediated by Kir4.1 in cultured rat cortical astrocytes. *J. Neurochem.***98,** 430-45
54. Hamill O.P., Marty A., Neher E., Sakmann B., Sigworth F.J. (1981) Improved patch-clamp techniques for high-resolution current recording from cells and cell-free membrane patches. *Pflugers Arch.***391,** 85-100
55. Amiry-Moghaddam M., Xue R., Haug F.M., Neely J.D., Bhardwaj A., Agre P., Adams M.E., Froehner S.C., Mori S., Ottersen O.P. (2004) Alpha-syntrophin deletion removes the perivascular but not endothelial

pool of aquaporin-4 at the blood-brain barrier and delays the development of brain edema in an experimental model of acute hyponatremia. *Faseb J.***18,** 542-4

56. Prydz A., Stahl K., Puchades M., Davarpaneh N., Nadeem M., Ottersen O.P., Gundersen V., Amiry-Moghaddam M. (2017) Subcellular expression of aquaporin-4 in substantia nigra of normal and MPTP-treated mice. *Neuroscience***359,** 258-266
57. Mola M.G., Nicchia G.P., Svelto M., Spray D.C., Frigeri A. (2009) Automated cell-based assay for screening of aquaporin inhibitors. *Anal. Chem.***81,** 8219-29
58. Mola M.G., Sparaneo A., Gargano C.D., Spray D.C., Svelto M., Frigeri A., Scemes E.,Nicchia G.P. (2016) The speed of swelling kinetics modulates cell volume regulation and calcium signaling in astrocytes: A different point of view on the role of aquaporins. *Glia***64,** 139-54
59. Sirianant L., Wanitchakool P., Ousingsawat J., Benedetto R., Zormpa A., Cabrita I., Schreiber R., Kunzelmann K. (2016) Non-essential contribution of LRRC8A to volume regulation. *Pflugers Arch.***468,** 805-16
60. Decher N., Lang H.J., Nilius B., Brüggemann A., Busch A.E., Steinmeyer K. (2001) DCPIB is a novel selective blocker of I(Cl,swell) and prevents swelling-induced shortening of guinea-pig atrial action potential duration. *Br. J. Pharmacol.***134,** 1467-79
61. Suadicani S.O., Brosnan C.F., Scemes E. (2006) P2X7 receptors mediate ATP release and amplification of astrocytic intercellular Ca^{2+} signaling. *J. Neurosci.***26,** 1378-85
62. Davidson J.S., Baumgarten I.M. (1988) Glycyrrhetinic acid derivatives: a novel class of inhibitors of gap-junctional intercellular communication. Structure-activity relationships. *J. Pharmacol. Exp. Ther*.**246,** 1104-7
63. Locovei S., Bao L., Dahl G. (2003) Pannexin 1 in erythrocytes: function without a gap. *Proc. Natl. Acad. Sci.* U.S.A.**103,** 7655-9
64. Bruzzone R., Hormuzdi S.G., Barbe M.T., Herb A., Monyer H. (2003) Pannexins, a family of gap junction proteins expressed in brain. *Proc. Natl. Acad. Sci. U.S.A.**100,*** 13644-9
65. Bruzzone R., Barbe M.T., Jakob N.J., Monyer H. (2005) Pharmacological properties of homomeric and heteromeric pannexin hemichannels expressed in Xenopus oocytes. *J. Neurochem.**92,*** 1033-43
66. Minieri L., Pivonkova H., Caprini M., Harantova L., Anderova M., Ferroni S. (2013) The inhibitor of volume-regulated anion channels DCPIB activates TREK potassium channels in cultured astrocytes. *Br. J. Pharmacol.***168,** 1240-54
67. Vessey J.P., Lalonde M.R., Mizan H.A., Welch N.C., Kelly M.E., Barnes S. (2004) Carbenoxolone inhibition of voltage-gated Ca channels and synaptic transmission in the retina. *J. Neurophysiol.***92,** 1252-6

68. Cardin V, Peña-Segura C, Pasantes-Morales H. Activation and inactivation of taurine efflux in hyposmoticand isosmotic swelling in cortical astrocytes: role of ionic strength and cell volume decrease. J Neurosci Res. 1999 Jun 15;56(6):659-67. PubMed PMID: 10374821.
69. Cardin V, Lezama R, Torres-Márquez ME, Pasantes-Morales H. Potentiation of the osmosensitive taurine release and cell volume regulation by cytosolic Ca2+ rise in cultured cerebellar astrocytes. Glia. 2003 Nov;44(2):119-28.
70. Haskew-Layton RE, Mongin AA, Kimelberg HK. Hydrogen peroxide potentiates volume-sensitive excitatory amino acid release via a mechanism involving Ca2+/calmodulin-dependent protein kinase II. J Biol Chem. 2005 Feb 4;280(5):3548-54. Epub 2004 Nov 29.
71. Benfenati, V., and Ferroni, S. (2015) Microdynamics of Water and Ion Homeostasis in the Brain. In *Homeostatic Control of Brain Function* (Boison, D., and Masino, S.A., eds) pp. 3-30, Oxford University Press, Oxford, England
72. Schober A.L., Wilson C.S., Mongin A.A. (2017) Molecular composition and heterogeneity of the LRRC8-containing swelling-activated osmolyte channels in primary rat astrocytes. *J. Physiol.***595,** 6939-6951
73. Barron K.D., Dentinger M.P., Kimelberg H.K., Nelson L.R., Bourke R.S., Keegan S., Mankes R., Cragoe E.J. Jr (1988) Ultrastructural features of a brain injury model in cat. I. Vascular and neuroglial changes and the prevention of astroglial swelling by a fluorenyl (aryloxy) alkanoic acid derivative (L-644,711). *Acta Neuropathol. (Berl)***75,** 595–307
74. Fabene P.F., Weiczner R., Marzola .P, Nicolato E., Calderan L., Andrioli A., Farkas E., Sule Z., Mihaly A., Sbarbati A. (2006) Structural and functional MRI following 4-aminopyridine-induced seizures: a comparative imaging and anatomical study. *Neurobiol. Dis.***21,** 80–89
75. Manley G.T., Fujimura M., Ma T., Noshita N., Filiz F., Bollen A.W., Chan P., Verkman A.S. (2000) Aquaporin-4 deletion in mice reduces brain edema after acute water intoxication and ischemic stroke. *Nat. Med.***6,** 159–163
76. Kimelberg H.K. (1995) Current concepts of brain edema. Review of laboratory investigations. *J. Neurosurg.***83,** 1051–1059
77. Amiry-Moghaddam M., Frydenlund D.S., Ottersen O.P. Anchoring of aquaporin-4 in brain: molecular mechanisms and implications for the physiology and pathophysiology of water transport. *Neuroscience***129,** 999-1010
78. Russell J.M. (2000) Sodium-potassium-chloride cotransport. *Physiol. Rev.***80,** 211-76
79. Benfenati V., Caprini M., Dovizio M., Mylonakou M.N., Ferroni S., Ottersen O.P., Amiry-Moghaddam M. (2011) An aquaporin-4/transient receptor potential vanilloid 4 (AQP4/TRPV4) complex is essential for cell-volume control in astrocytes. *Proc. Natl. Acad. Sci. U. S .A.***108,** 2563-8

80. Benfenati V., Amiry-Moghaddam M., Caprini M., Mylonakou M.N., Rapisarda C., Ottersen O.P., Ferroni S. (2007) Expression and functional characterization of transient receptor potential vanilloid-related channel 4 (TRPV4) in rat cortical astrocytes. *Neuroscience***148,** 876-92
81. Nielsen S., Nagelhus E.A., Amiry-Moghaddam M., Bourque C., Agre P., Ottersen O.P. (1997) Specialized membrane domains for water transport in glial cells: high-resolution immunogold cytochemistry of aquaporin-4 in rat brain. *J. Neurosci*.**17,** 171-80
82. Papadopoulos M.C., Verkman A.S. (2013) Aquaporin water channels in the nervous system. *Nat. Rev. Neurosci*.**14,** 265-77
83. Nilius B. (2004) Is the volume-regulated anion channel VRAC a "water-permeable" channel? *Neurochem. Res*.**29,** 3-8

Figure 1

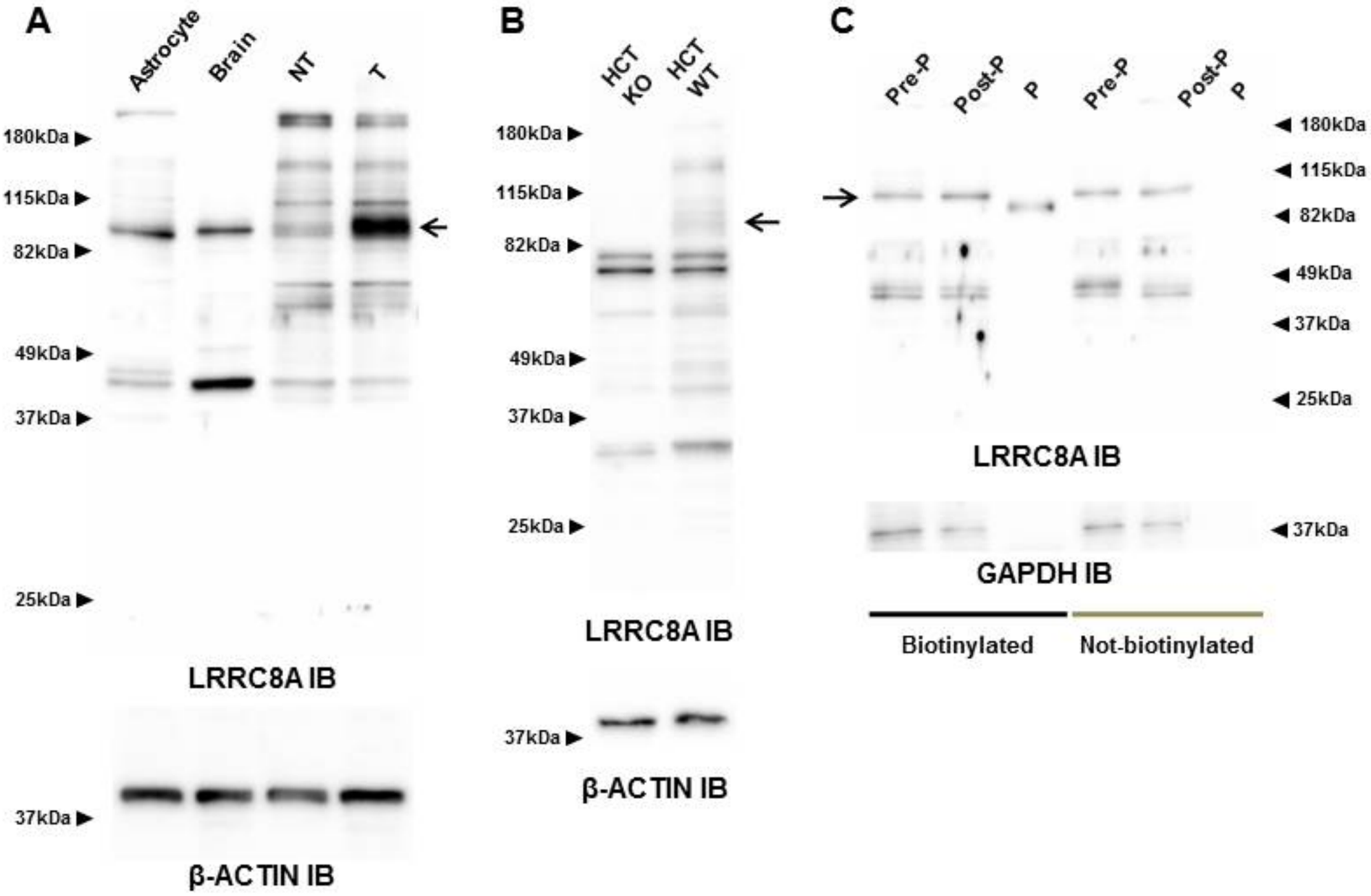

Figure 1

Figure 2

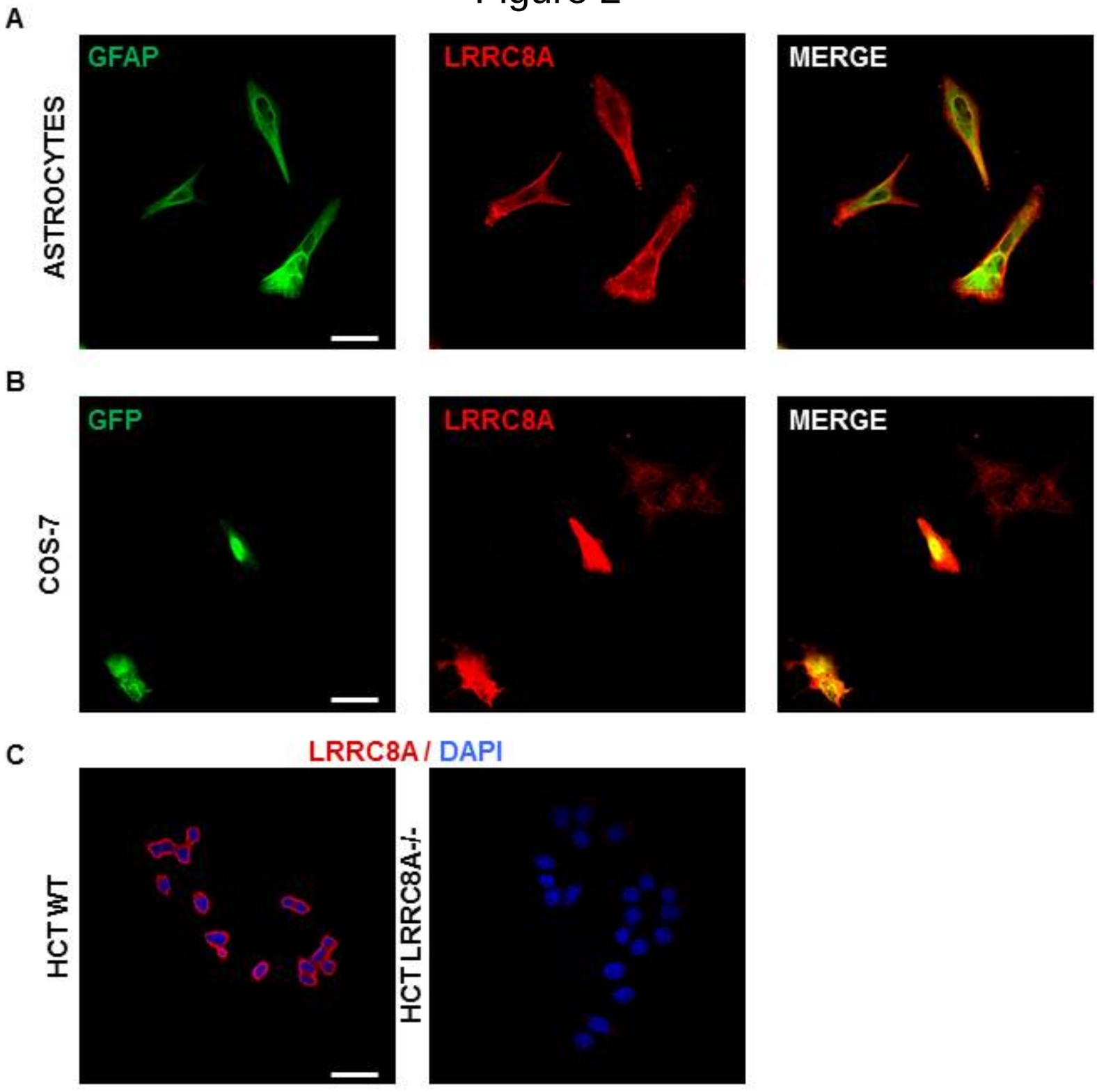

Figure 2

Figure 3

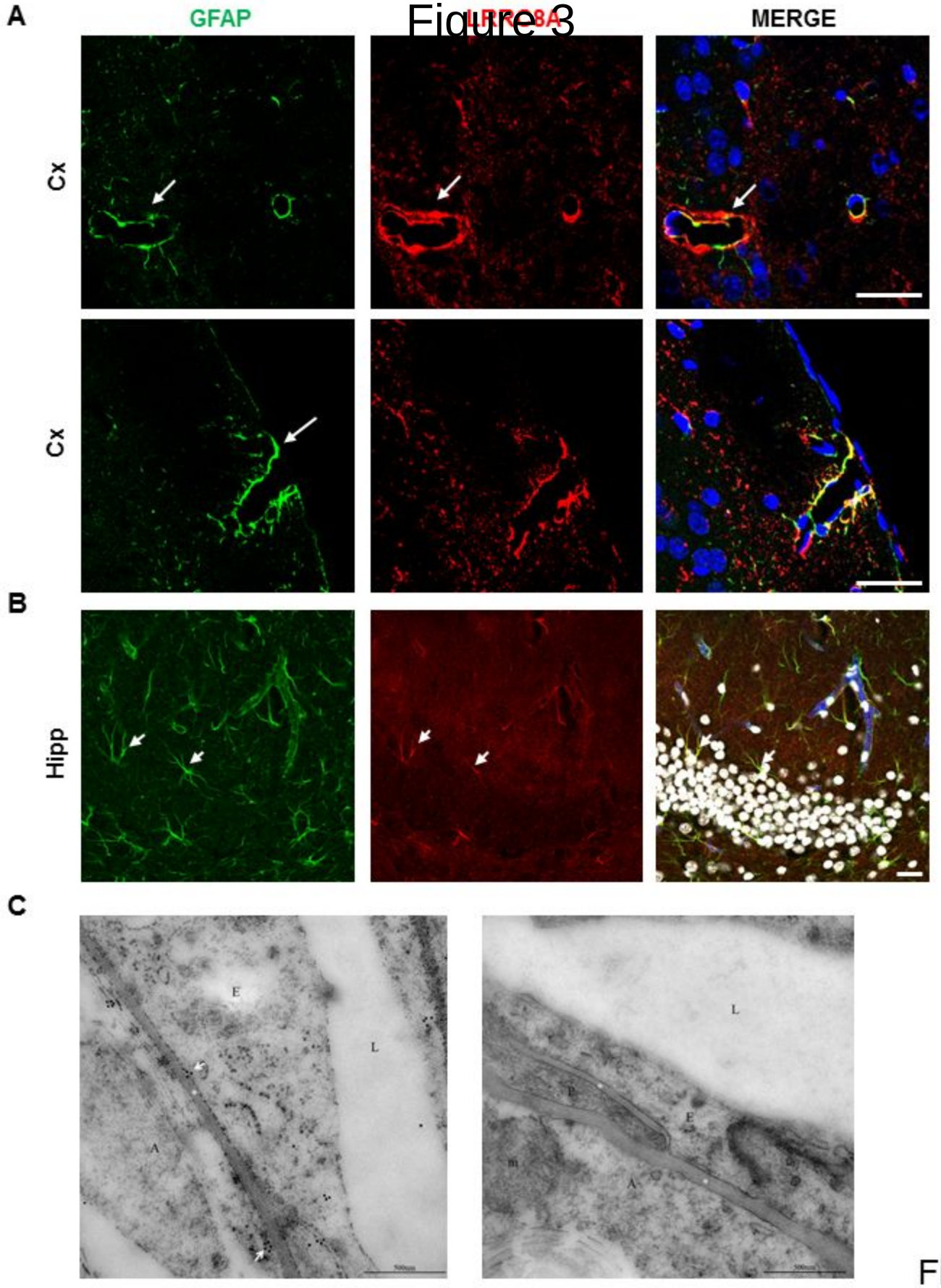

Figure 3

Figure 4

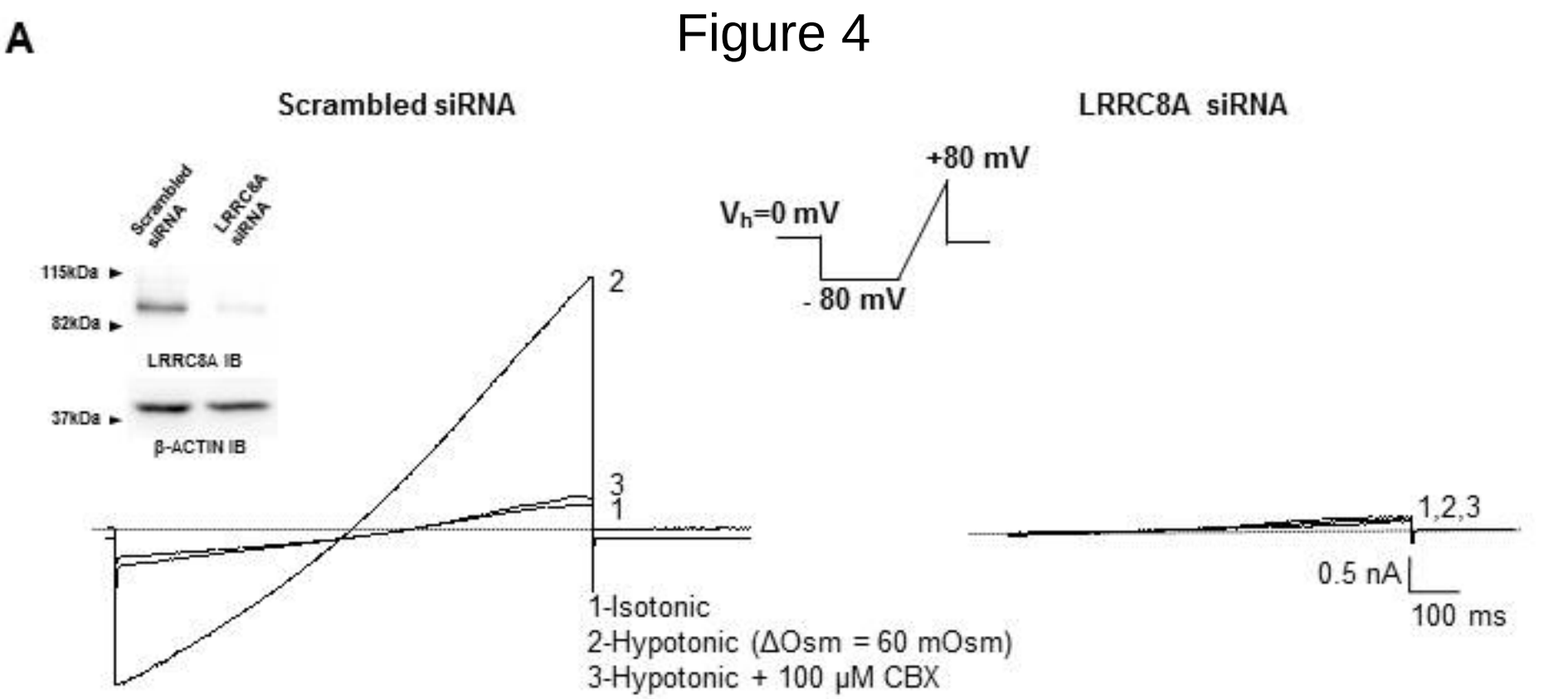

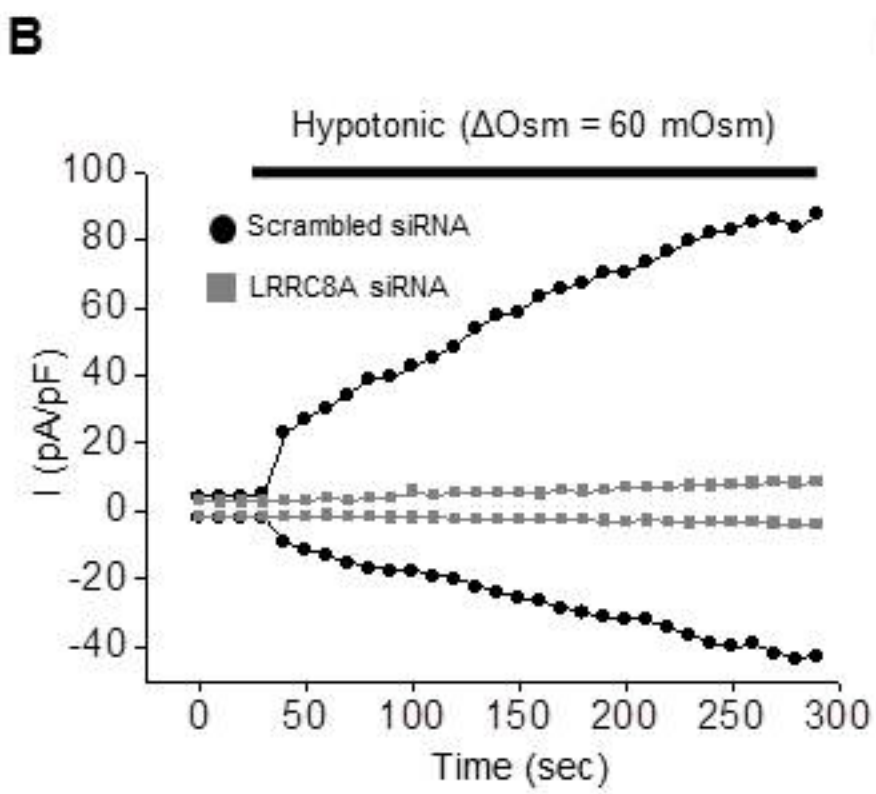

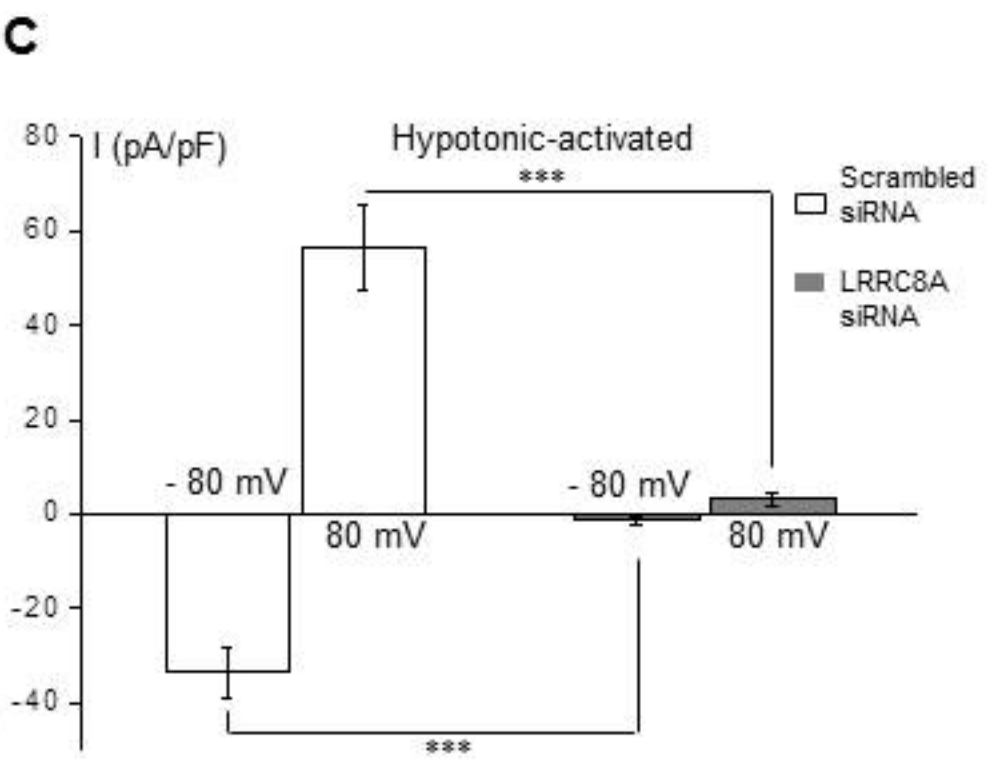

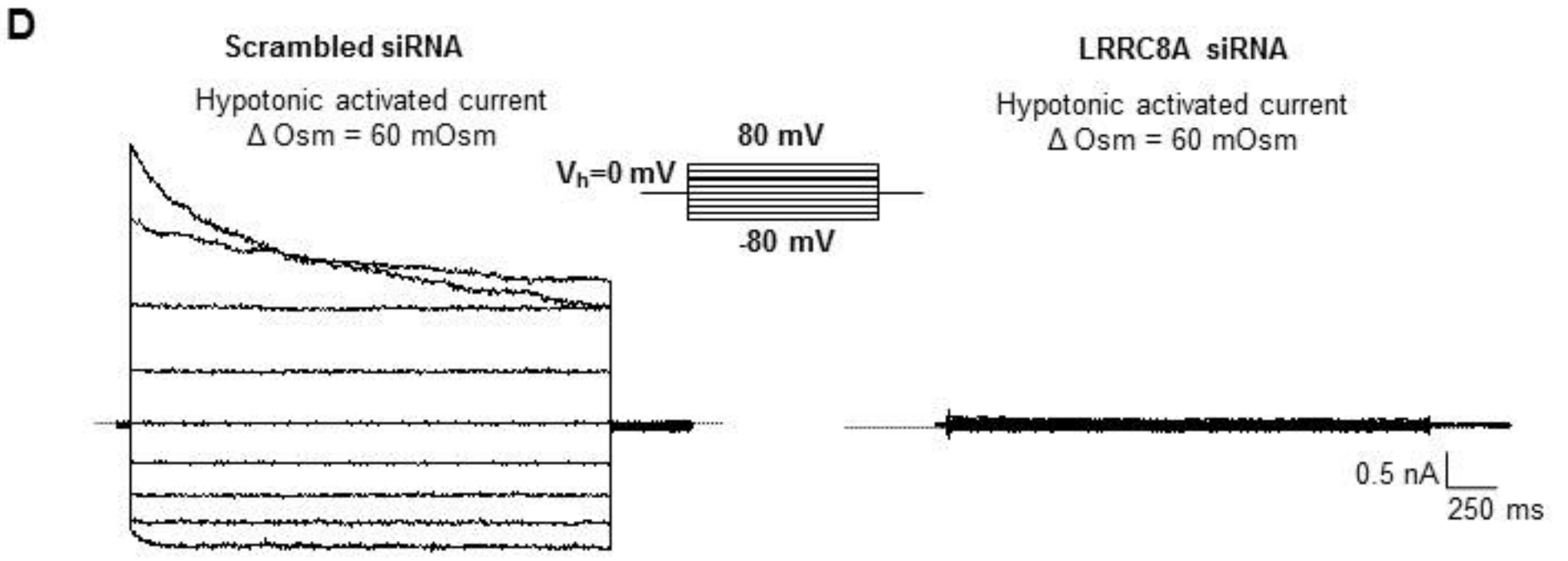

Figure 4

Figure 5

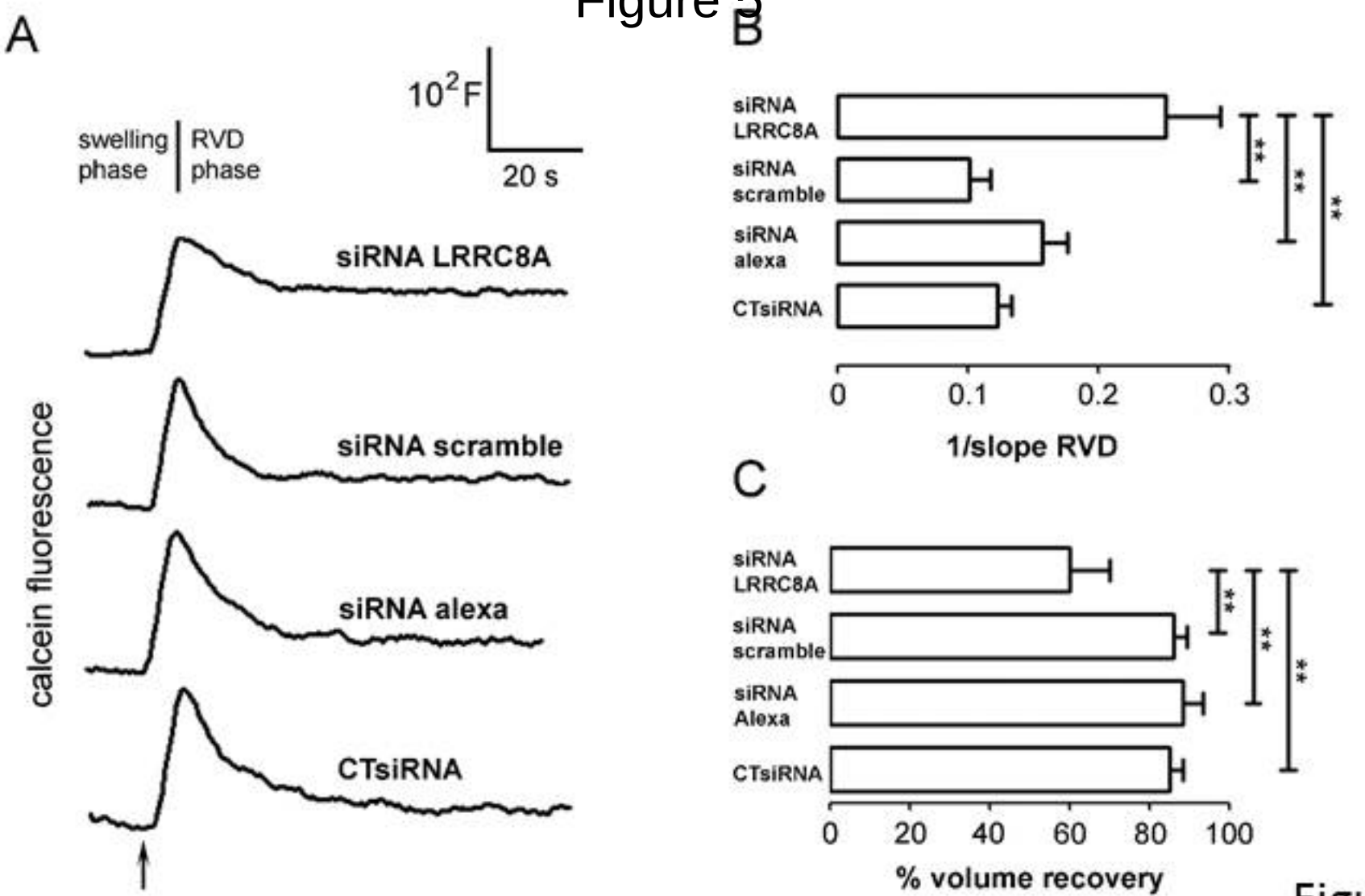

Figure 5

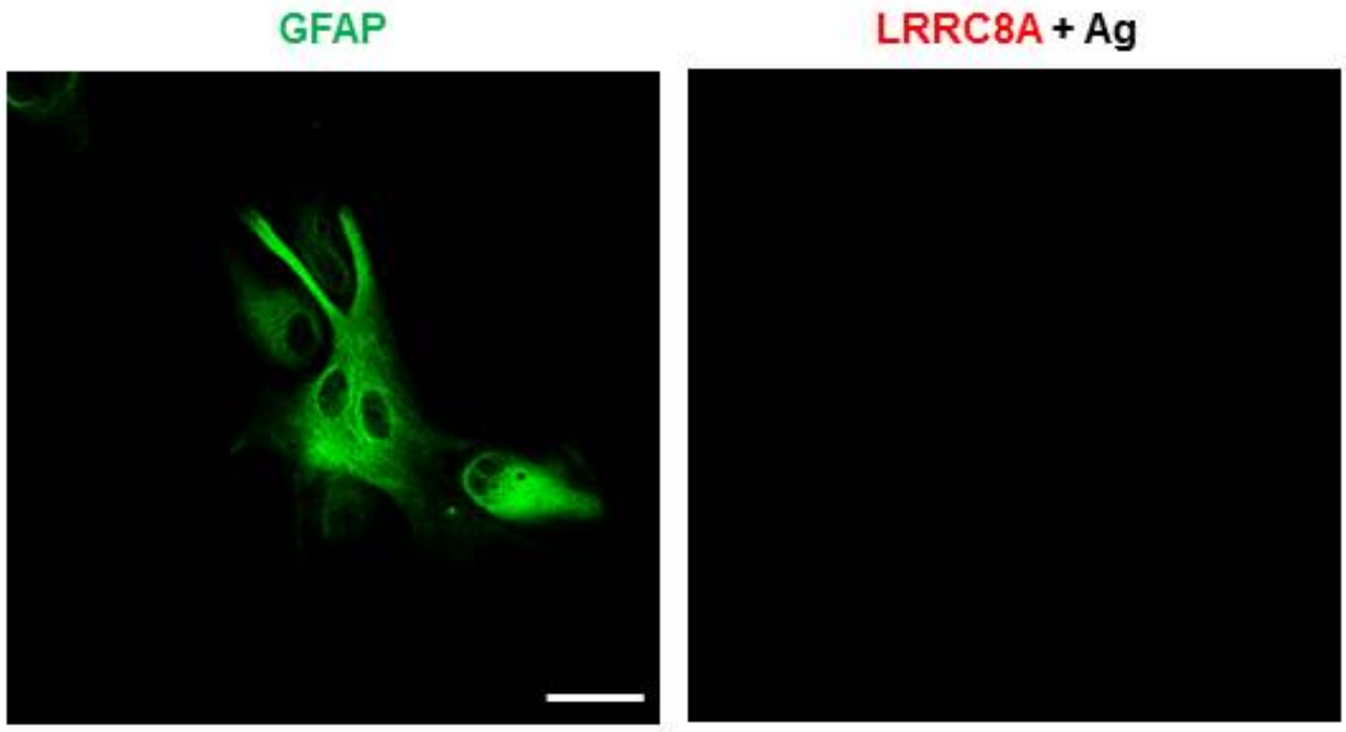

Single plane confocal immunofluorescence image of primary rat cortical astrocytes co-immunolabeled for Glial Fibrillary Acidic Protein (GFAP, left panel, green) and LRRC8A. Anti-LRRC8A was pre-adsorbed by incubation with immunizing peptide (right panel, red). Scale: 50 μm

Supporting Material S1

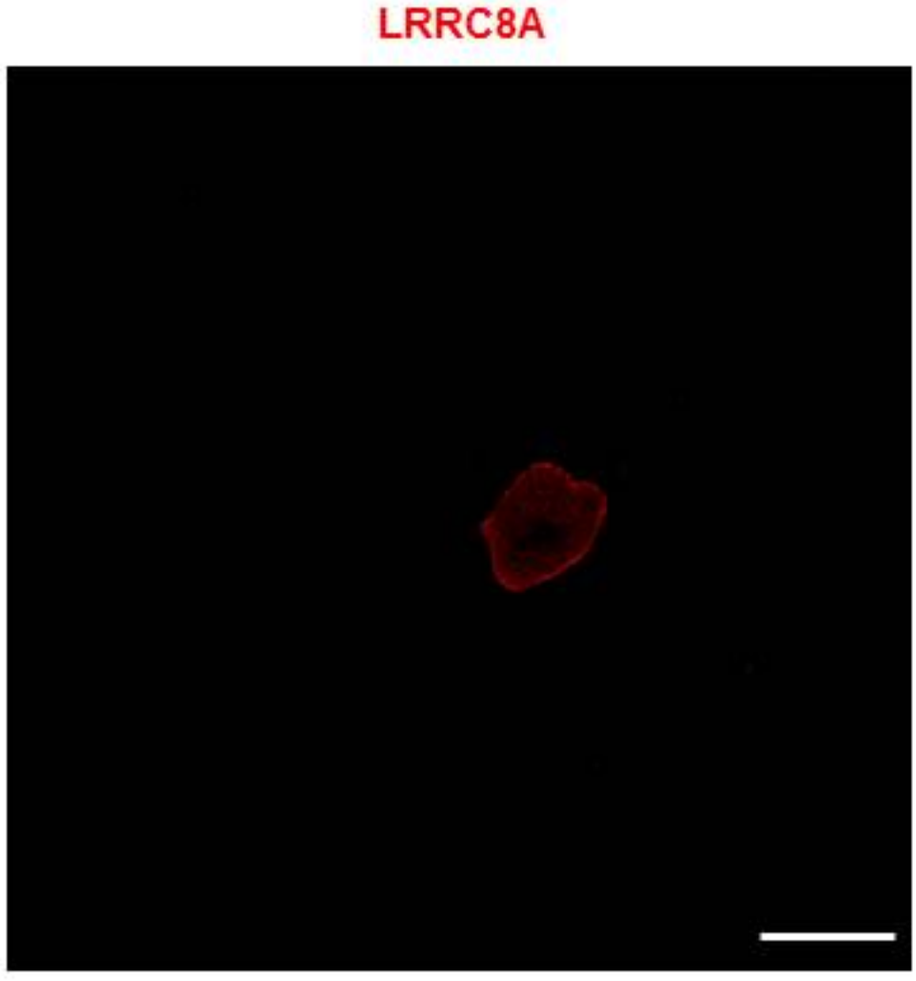

Immunostaining of LRRC8A (red) in single plane confocal images of naïve COS-7 Scale: 50 µm

Supporting Material S2

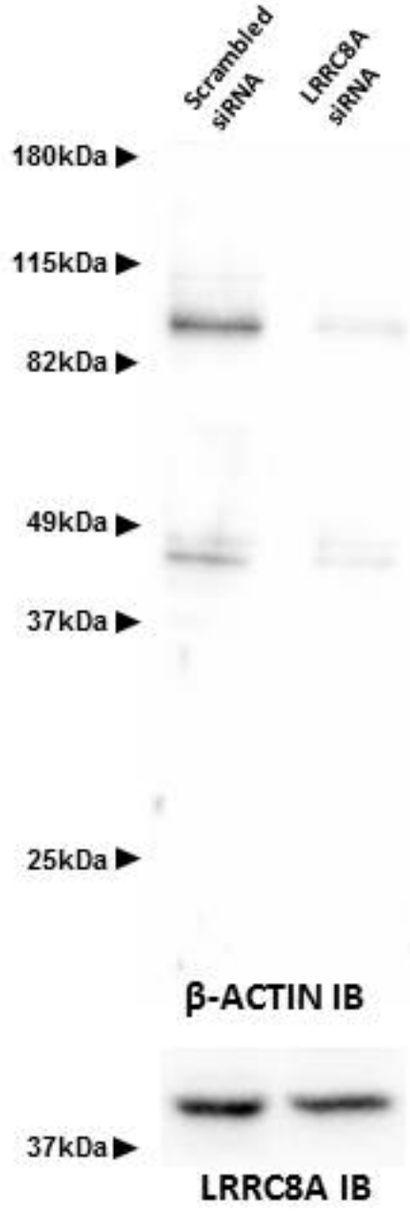

Western blot analysis of astrocytes transfected with LRRC8A siRNA and Scramble siRNA. Full lane image releated to the inset in Fig. 4 A

Supporting Material S3

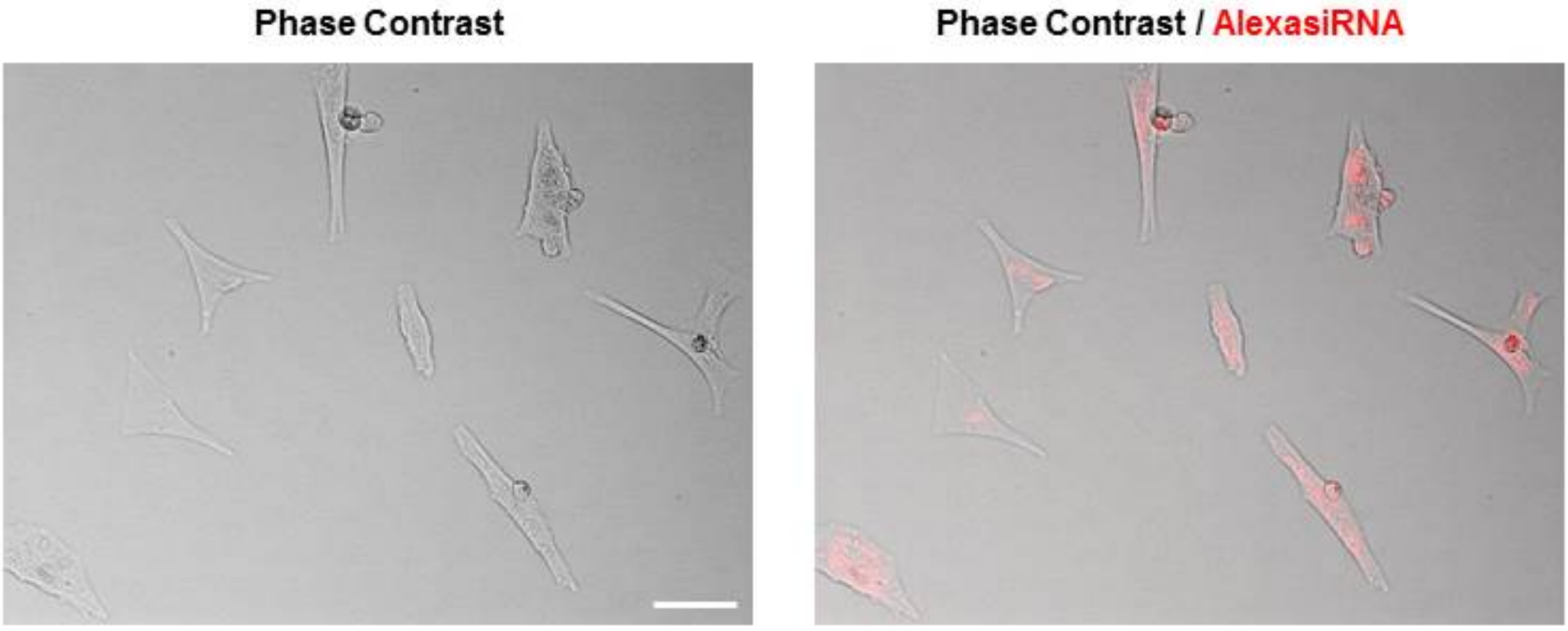

Sub-confluent astrocytes transfected with AlexasiRNA, 48 h after transfection. On the left panel phase contrast image is depicted. On the right the merged image with AlexasiRNA fluorescent signal. The transfection efficiency routinely reached 95%. Scale: 80 μm

Supporting Material S4

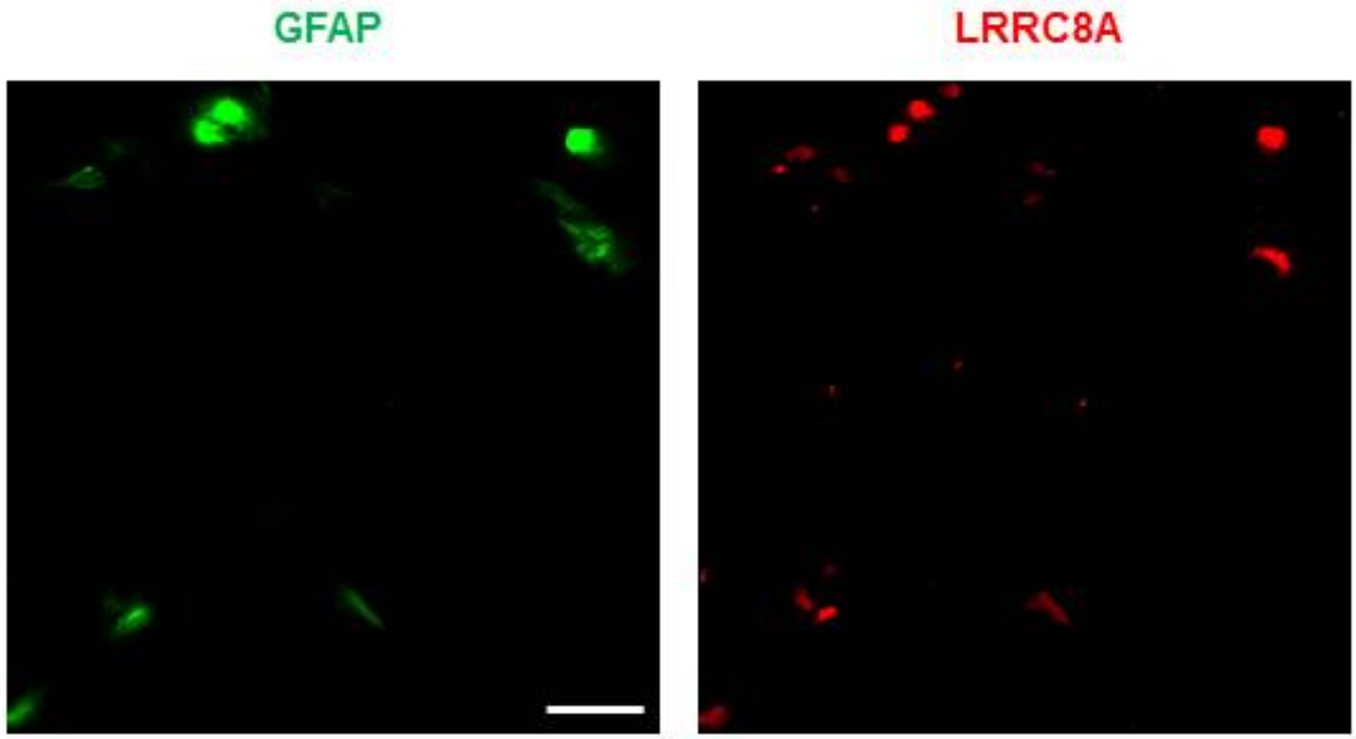

Single plane confocal immunofluorescence image of primary rat cortical astrocytes co-stained for Glial Fibrillary Acidic Protein (GFAP, left panel, green) and LRRC8A (right panel, red). Detergents were omitted from the preparation. Scale: 50 μm

Supporting Material S5

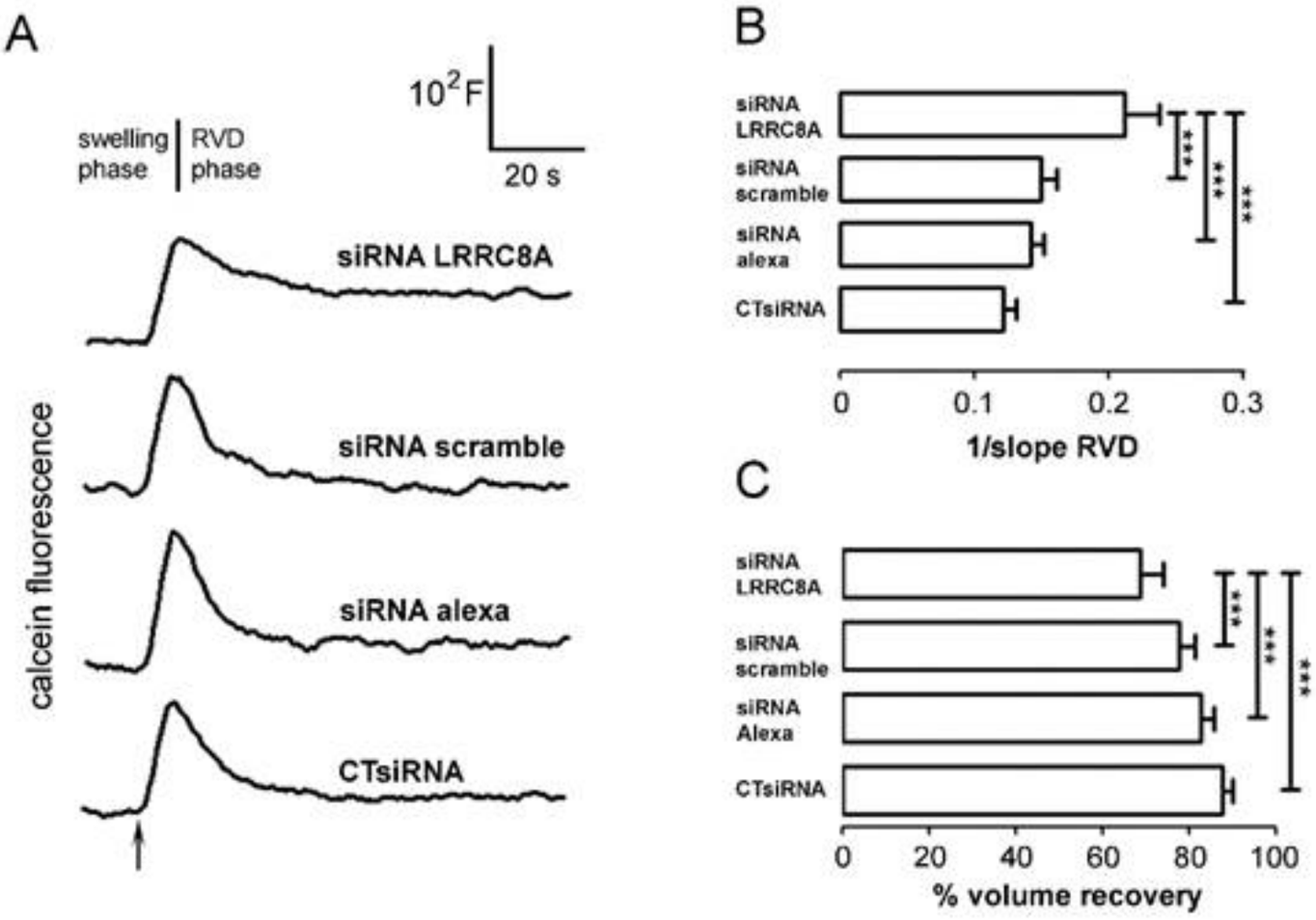

RVD kinetic in rat astrocytes challenged with hypotonic solution ΔOsm = 25 mOsm (A) Osmotically-induced volume changes recordered by calcein quenching method in primary rat astrocytes treated with CTsiRNA, Alexa siRNA, scramble siRNA and LRRC8AsiRNA. The arrow indicates the addition of a hypotonic solution (ΔOsm = 25 mOsm). (B) Histogram of the mean ± SE values of 1/slope values of the RVD phase of the indicated cells calculated by linear regression of the experimental data. (C) Histogram showing the mean ± SE of the extent of volume recovery (in percent). ***$p < 0.001$; **$p< 0.01$; *$p< 0.05$; n=16 for LRRC8A-specific siRNA; n=19 for Alexa siRNA; n=19 for control siRNA; n=19 scramble siRNA.

Supporting Material S6